JOURNAL OF VIROLOGY, Mar. 2009, p. 2338–2348 Vol. 83, No. 5
0022-538X/09/$08.00+0 doi:10.1128/JVI.01840-08

Arsenic Trioxide Inhibits Hepatitis C Virus RNA Replication through Modulation of the Glutathione Redox System and Oxidative Stress▽

Misao Kuroki,[1] Yasuo Ariumi,[1] Masanori Ikeda,[1] Hiromichi Dansako,[1] Takaji Wakita,[2] and Nobuyuki Kato[1]*

Department of Tumor Virology, Okayama University Graduate School of Medicine, Dentistry, and Pharmaceutical Sciences, 2-5-1, Shikata-cho, Okayama 700-8558, Japan,[1] and Department of Virology II, National Institute of Infectious Diseases, 1-23-1 Toyama, Shinjuku-ku, Tokyo 162-8640, Japan[2]

Received 2 September 2008/Accepted 13 December 2008

Arsenic trioxide (ATO), a therapeutic reagent used for the treatment of acute promyelocytic leukemia, has recently been reported to increase human immunodeficiency virus type 1 infectivity. However, in this study, we have demonstrated that replication of genome-length hepatitis C virus (HCV) RNA (O strain of genotype 1b) was notably inhibited by ATO at submicromolar concentrations without cell toxicity. RNA replication of HCV-JFH1 (genotype 2a) and the release of core protein into the culture supernatants were also inhibited by ATO after the HCV infection. To clarify the mechanism of the anti-HCV activity of ATO, we examined whether or not PML is associated with this anti-HCV activity, since PML is known to be a target of ATO. Interestingly, we observed the cytoplasmic translocation of PML after treatment with ATO. However, ATO still inhibited the HCV RNA replication even in the PML knockdown cells, suggesting that PML is dispensable for the anti-HCV activity of ATO. In contrast, we found that *N*-acetyl-cysteine, an antioxidant and glutathione precursor, completely and partially eliminated the anti-HCV activity of ATO after 24 h and 72 h of treatment, respectively. In this context, it is worth noting that we found an elevation of intracellular superoxide anion radical, but not hydrogen peroxide, and the depletion of intracellular glutathione in the ATO-treated cells. Taken together, these findings suggest that ATO inhibits the HCV RNA replication through modulation of the glutathione redox system and oxidative stress.

Hepatitis C virus (HCV) is the causative agent of chronic hepatitis, which progresses to liver cirrhosis and hepatocellular carcinoma. HCV is an enveloped virus with a positive single-stranded 9.6-kb RNA genome, which encodes a large polyprotein precursor of approximately 3,000 amino acid residues. This polyprotein is cleaved by a combination of the host and viral proteases into at least 10 proteins in the following order: core, envelope 1 (E1), E2, p7, nonstructural 2 (NS2), NS3, NS4A, NS4B, NS5A, and NS5B (30).

Alpha interferon has been used as an effective anti-HCV reagent in clinical therapy for patients with chronic hepatitis C. The current combination treatment with pegylated alpha interferon and ribavirin, a nucleoside analogue, has been shown to improve the sustained virological response rate to more than 50% (15). However, the adverse effects of the combination therapy and the limited efficacy against genotype 1b warrant the development of new anti-HCV reagents.

Arsenic trioxide (ATO) (As_2O_3, arsenite) has been used as a therapeutic reagent in acute promyelocytic leukemia, which bears an oncogenic PML-retinoic acid receptor alpha fusion protein resulting from chromosomal translocation (51, 52, 68, 70). The ATO treatment induces complete remission through degradation of the aberrant PML-retinoic acid receptor α (70). The PML tumor suppressor protein is required for formation of the PML nuclear body (PML-NB), also known as nuclear dot 10 or the PML oncogenic domain, which is often disrupted by infection with DNA viruses, such as herpes simplex virus type 1, human cytomegalovirus, and Epstein-Barr virus (17). The treatment with ATO results in degradation of the PML protein and disruption of the PML-NB (70). Therefore, ATO has been become a useful probe for investigating the functions of the PML-NB, including cell growth, apoptosis, stress response, and viral infection. Indeed, ATO has been shown to increase retroviral infectivity, such as human immunodeficiency virus type 1 (HIV-1) and murine leukemia virus infectivity, but the mechanisms of this change are not well understood (5, 6, 32, 44, 47, 50, 57). In contrast, ATO was recently reported to inhibit the replication of HCV subgenomic replicon RNA (24). However, it also remains unclear how ATO inhibits the HCV RNA replication. In this study, using genome-length HCV RNA replication systems, we investigated the molecular mechanism(s) of the anti-HCV activity of ATO, and we provide evidence that ATO inhibits HCV RNA replication through modulation of the glutathione redox system and oxidative stress.

MATERIALS AND METHODS

Reagents. ATO, *N*-acetyl-cysteine (NAC), ascorbic acid (vitamin C), and L-buthionine sulfoximine (BSO) were purchased from Sigma (St. Louis, MO). Arsenic pentoxide (APO) (As_2O_5, arsenate) was purchased from Wako (Osaka, Japan). Both ATO and APO were dissolved in 1 N NaOH at 0.1 M as a stock solution. An inducible nitric oxide synthase (iNOS) inhibitor, 1400W, was purchased from Calbiochem (Merck Biosciences, Darmstadt, Germany).

Cell culture. 293FT cells were cultured in Dulbecco's modified Eagle's medium (Invitrogen, Carlsbad, CA, USA) supplemented with 10% fetal bovine serum. The following four HuH-7-derived cell lines or their parental HuH-7 cells

* Corresponding author. Mailing address: Department of Tumor Virology, Okayama University Graduate School of Medicine, Dentistry, and Pharmaceutical Sciences, 2-5-1, Shikata-cho, Okayama 700-8558, Japan. Phone: 81 86 235 7385. Fax: 81 86 235 7392. E-mail: nkato@md.okayama-u.ac.jp.

▽ Published ahead of print on 24 December 2008.

were cultured in Dulbecco's modified Eagle's medium with 10% fetal bovine serum as described previously (25): O cells, harboring a replicative genome-length HCV-O RNA (O strain of genotype 1b) (25); OR6 cells, harboring the genome-length HCV-O RNA with luciferase as a reporter (25); sO cells, harboring the subgenomic replicon RNA of HCV-O (31); and RSc cured cells, which cell culture-generated HCV-JFH1 (JFH1 strain of genotype 2a) (58) could infect and effectively replicate in (2, 3). The O, OR6, and sO cells were maintained in the presence of G418 (300 μg/ml Geneticin; Invitrogen).

RNA interference. Oligonucleotides with the following sense and antisense sequences were used for the cloning of short hairpin RNA (shRNA)-encoding sequences targeted to PML (56) in a lentiviral vector: 5′-GATCCCCAGATGC AGCTGTATCCAAGTTCAAGAGACTTGGATACAGCTGCATCTTTTTTG GAAA-3′ (sense) and 5′-AGCTTTTCCAAAAAAGATGCAGCTGTATCCAA GTCTCTTGAACTTGGATACAGCTGCATCTGGG-3′ (antisense). These oligonucleotides were annealed and subcloned into the BglII-HindIII site, downstream from an RNA polymerase III promoter of pSUPER (8), to generate pSUPER-PMLi. To construct pLV-PMLi, the BamHI-SalI fragments of pSUPER-PMLi were subcloned into the BamHI-SalI site of pRDI292, an HIV-1-derived self-inactivating lentiviral vector containing a puromycin resistance marker allowing for the selection of transduced cells (7). pLV-Chk2i was described previously (3).

Lentiviral vector production. The vesicular stomatitis virus (VSV) G-pseudotyped HIV-1-based vector system has been described previously (42). The lentiviral vector particles were produced by transient transfection of the second-generation packaging construct pCMV-ΔR8.91 (1, 71) and the VSV G envelope-expressing plasmid pMDG2 as well as pRDI292 into 293FT cells with FuGene6 (Roche Diagnostics, Mannheim, Germany).

HCV infection experiments. The supernatants was collected from cell culture-generated HCV-JFH1 (58)-infected RSc cells (2, 3) at 5 days postinfection and stored at −80°C after filtering through a 0.45-μm filter (Kurabo, Osaka, Japan) until use. For infection experiments with HCV-JFH1 virus, RSc cells (1×10^5 cells/well) were plated onto six-well plates and cultured for 24 h. We then infected the cells with 50 μl (equivalent to a multiplicity of infection of 0.05 to 0.1) of inoculum. The culture supernatants were collected at 97 h postinfection, and the levels of the core protein were determined by enzyme-linked immunosorbent assay (Mitsubishi Kagaku Bio-Clinical Laboratories, Tokyo, Japan). Total RNA was isolated from the infected cellular lysates using an RNeasy minikit (Qiagen, Hilden, Germany) for quantitative reverse transcription-PCR (RT-PCR) analysis of intracellular HCV RNA. The level of intracellular HCV RNA in the RSc cells was $>10^8$ copies/μg total RNA at 4 days postinfection.

Quantitative RT-PCR Analysis. The quantitative RT-PCR analysis for HCV RNA was performed by real-time LightCycler PCR (Roche) as described previously (25). We used the following forward and reverse primer sets for the real-time LightCycler PCR: PML, 5′-GAGGAGTTCCAGTTTCTGCG-3′ (forward), 5′-GCGCCTGGCAGATGGGGCAC-3′ (reverse); β-actin, 5′-TGACGG GGTCACCCACACTG-3′ (forward), 5′-AAGCTGTAGCCGCGCTCGGT-3′ (reverse); HCV-O, 5′-AGAGCCATAGTGGTCTGCGG-3′ (forward), 5′-CTT TCGCGACCCAACACTAC-3′ (reverse); and HCV-JFH1, 5′-5′-AGAGCCAT AGTGGTCTGCGG-3′ (forward), 5′-CTTTCGCAACCCAACGCTAC-3′ (reverse).

Western blot analysis. Cells were lysed in buffer containing 50 mM Tris-HCl (pH 8.0), 150 mM NaCl, 4 mM EDTA, 1% Nonidet P-40, 0.1% sodium dodecyl sulfate, 1 mM dithiothreitol, and 1 mM phenylmethylsulfonyl fluoride. Supernatants from these lysates were subjected to sodium dodecyl sulfate-polyacrylamide gel electrophoresis, followed by immunoblot analysis using anti-PML (A301-168A-1; Bethyl Laboratories, Montgomery, TX), anti-Chk2 (DCS-273; Medical & Biological Laboratories, MBL, Nagoya, Japan), anti-HCV core (CP-9 and CP-11; Institute of Immunology, Tokyo, Japan), anti-HCV NS5A (no. 8926; a generous gift from A Takamizawa, The Research Foundation for Microbial Diseases of Osaka University, Japan), anti-signal transducer and activator of transcription 3 (anti-STAT3) (BD Bioscience, San Jose, CA), anti-phospho-STAT3 (Tyr705) (Cell Signaling Technology, Danvers, MA) anti-poly(ADP-ribose) polymerase 1 (anti-PARP-1) (C-2-10; Calbiochem), or anti-β-actin antibody (Sigma).

MTT assay. HuH-7 or O cells (5×10^3 cells/well) were plated onto 96-well plates and cultured for 24 h. The cells were treated with ATO, APO, or NaOH for 24, 48, or 72 h and then subjected to the colorimetric 3-(4,5-dimethylthiazol-2-yl)-2,5-diphenyltetrazolium bromide (MTT) assay according to the manufacturer's instructions (cell proliferation kit I; Roche). The absorbance was read using a microplate reader (model 2550; Bio-Rad Laboratories, Hercules, CA) at 550 nm with a reference wavelength of 690 nm.

RL assay. OR6 cells (1.5×10^4 cells/well) were plated onto 24-well plates and cultured for 24 h. The cells were treated with each reagent for 72 h and then subjected to the *Renilla* luciferase (RL) assay according to the manufacturer's instructions (Promega, Madison, WI). A Lumat LB9507 luminometer (Berthold, Bad Wildbad, Germany) was used to detect RL activity.

FL assay. Plasmids were transfected into O cells (2×10^4 cells/well in 24-well plates) using FuGene6 and cultured for 24 h. The cells were treated with or without 1 μM ATO for 24 h, and then firefly luciferase (FL) assays were performed according to the manufacturer's instructions (Promega).

Immunofluorescence and confocal microscopic analysis. Cells were fixed in 3.6% formaldehyde in phosphate-buffered saline (PBS), permeabilized in 0.1% NP-40 in PBS at room temperature, and incubated with anti-PML antibody (PM001; MBL) at a 1:300 dilution in PBS containing 3% bovine serum albumin at 37°C for 30 min. They were then stained with fluorescein isothiocyanate-conjugated anti-rabbit antibody (Jackson ImmunoResearch, West Grove, PA) at a 1:300 dilution in PBS containing bovine serum albumin at 37°C for 30 min, followed by staining with 4′,6-diamidino-2-phenylindole (DAPI) at room temperature for 15 min. Following extensive washing in PBS, the cells were mounted on slides using a mounting medium of 90% glycerin–10% PBS with 0.01% *p*-phenylenediamine added to reduce fading. Samples were viewed under a confocal laser-scanning microscope (LSM510; Zeiss, Jena, Germany).

Measurement of intracellular O_2^- and H_2O_2 production. The intracellular superoxide anion radical (O_2^-) levels were measured with an oxidation-sensitive fluorescent probe, dihydroethidium (DHE) (Invitrogen Molecular Probes), that is highly selective for detection of O_2^- among reactive oxygen species (ROS). DHE is cell permeative and reacts with O_2^- to form ethidium, which in turn intercalates in DNA, thereby exhibiting a red fluorescence. The intracellular hydrogen peroxide (H_2O_2) levels were measured with another oxidation-sensitive fluorescent probe dye, 6-carboxy-2′,7′-dichlorodihydrofluorescein diacetate (carboxy-H_2DCFDA) (Invitrogen Molecular Probes). Carboxy-H_2DCFDA was intracellularly deacetylated with esterase and further oxidized with peroxidase to the fluorescent 2′,7′-dichlorodihydrofluorescein (DCF). The ATO- or BSO-treated O cells were washed with PBS and incubated with 5 μM DHE and 20 μM carboxy-H_2DCFDA in PBS at 37°C for 30 min. Cells were then washed twice with PBS. The DHE or DCF fluorescence intensity was measured using a FACSCalibur flow cytometer. For each sample, 10,000 events were collected. The O_2^- or H_2O_2 levels are indicated as mean fluorescence intensities, which were determined with the CellQuest software (BD Bioscience).

Detection of intracellular glutathione. Intracellular glutathione levels were analyzed using CellTracker Green (5-chloromethylfluorescein diacetate [CMFDA]; Molecular Probes, Invitrogen). CMFDA is a membrane-permeative dye used to determine intracellular glutathione levels. Cytoplasmic esterase converts the nonfluorescent CMFDA to the fluorescent 5-chloromethylfluorescein (CMF), which can then react with glutathione. The excitation peak is at 492 nm, and the fluorescence emission peak is at 517 nm. O cells treated with 1 μM ATO for 72 h were washed with PBS and incubated with 5 μM CMFDA at 37°C for 30 min. The CMF fluorescence intensity was measured using a FACSCalibur flow cytometer. For each sample, 10,000 events were collected. The glutathione levels are given as the relative mean fluorescence intensities, which were determined with CellQuest software.

RESULTS

ATO inhibits HCV RNA replication. First, we quantitatively examined the effect of ATO on the HCV RNA replication in HuH-7-derived O cells harboring a replicative genome-length HCV-O RNA (25). We found that submicromolar concentrations of ATO markedly inhibited genome-length HCV-O RNA replication in the O cells at 72 h after administration (Fig. 1A). The 50% effective concentration (EC_{50}) of ATO required for inhibition of genome-length HCV-O RNA replication was 0.19 μM (Fig. 1A). Consistent with this finding, the expression levels of the HCV core and NS5A proteins were also significantly decreased in the cell lysates of O cells treated with ATO for 72 h (Fig. 1B). In addition, ATO markedly inhibited the replication of the subgenomic replicon RNA (31), with an EC_{50} of 0.48 μM at 72 h after the treatment (Fig. 1C). We next examined the effect of ATO on HCV reproduction by HCV-JFH1 infection (58). The results revealed that ATO significantly inhibited the intracellular RNA replication of HCV-

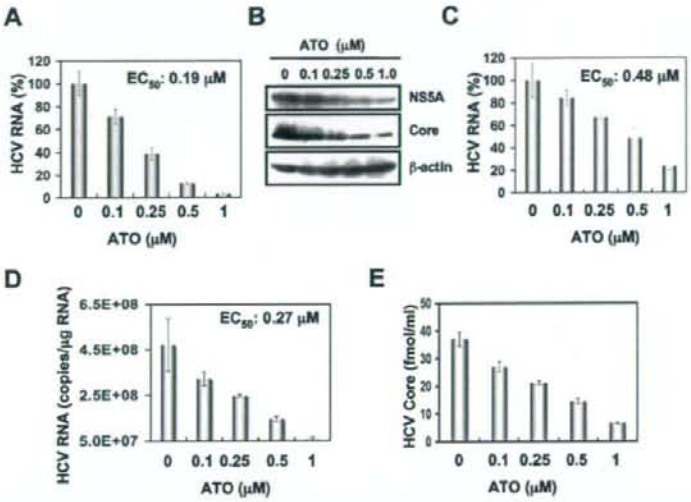

FIG. 1. Inhibition of HCV RNA replication by ATO. (A) The level of genome-length HCV RNA in O cells after the treatment with ATO was monitored by real-time LightCycler PCR. Experiments were done in triplicate and, bars represent the mean percentage of HCV RNA. Error bars indicate standard deviations. (B) HCV core and NS5A protein expression levels in O cells after treatment with ATO. The results of Western blot analysis of cellular lysates with anti-HCV core, anti-HCV NS5A, or anti-β-actin antibody in O cells at 72 h after treatment with ATO at the indicated concentration are shown. (C) The level of subgenomic replicon RNA was monitored by real-time LightCycler PCR. Results from three independent experiments conducted as described for panel A are shown. (D) The level of intracellular genome-length HCV-JFH1 RNA was monitored by real-time LightCycler PCR. RSc cells were pretreated with the indicated concentration of ATO for 13 h, followed by inoculation of the HCV-JFH1 virus, and then the infected cells were further incubated with ATO for 97 h. Results from three independent experiments conducted as described for panel A are shown. (E) The levels of the core protein in the culture supernatants treated as described for panel D were determined by enzyme-linked immunosorbent assay. Experiments were done in triplicate, and bars represent the mean core protein levels.

JFH1, with an EC_{50} of 0.27 μM, as well as the release of core protein into the culture supernatants in HuH-7-derived RSc cells at 97 h after inoculation of the HCV-JFH1 virus (Fig. 1D and E). Thus, we have demonstrated for the first time that ATO can inhibit the reproduction of HCV and particularly HCV RNA replication.

Effect of APO on HCV replication. Arsenic is known to exist in two oxidation states, As(III) in ATO and As(V) in APO. As ATO in the lower valence state has been reported to be more toxic than APO (48), we compared their anti-HCV activities using an OR6 assay system, which was recently developed as a luciferase reporter assay system for monitoring genome-length HCV RNA replication in HuH-7-derived OR6 cells (Fig. 2A) (25). The results showed that APO could not strongly suppress HCV replication at submicromolar concentrations, while ATO strongly inhibited it, with an EC_{50} of 0.33 μM (Fig. 2B and C), indicating that ATO has unique anti-HCV activity. In this context, it is relevant that the expression level of HCV core protein was also remarkably decreased in the cell lysates of O cells treated with ATO, but not those treated with APO, for 72 h (Fig. 2D). Thus, APO seems to be a useful negative probe to clarify the mechanism of the anti-HCV activity of ATO.

ATO does not affect cell growth at submicromolar concentrations. ATO has been reported to induce apoptosis (11, 14, 20, 21, 26–28, 33, 48, 66). Therefore, such an ATO-induced apoptosis may be involved in the anti-HCV activity. To test this possibility, we examined the effect of ATO or APO at various concentrations on cell proliferation by colorimetric MTT assay. In this context, we demonstrated that ATO did not affect the cell proliferation of O cells or the parental HCV-negative HuH-7 cells at submicromolar concentrations (Fig. 3A and E). In contrast, 4 or 8 μM ATO significantly inhibited cell proliferation (Fig. 3B and F). Similarly, APO did not affect the cell proliferation at less than 2 μM (Fig. 3C and D). Consistent with the above results, ATO-treated O cells exhibited normal growth rates and cell viabilities, at least at 1 μM for 72 h (Fig. 3G). Furthermore, we did not observe the cleavage of PARP-1, which is known to be an important substrate for activated caspase 3, in O cells treated with 1 μM ATO at least until 72 h (Fig. 3H), indicating that 1 μM ATO did not induce apoptosis in O cells. Thus, we concluded that the anti-HCV activity was independent of ATO-induced apoptosis or cell toxicity, at least at submicromolar concentrations.

PML and Chk2 are dispensable for the anti-HCV activity of ATO. Since PML is known to be a target of ATO (70), we first examined the subcellular localization of PML in O cells treated with either 1 μM ATO or 1 μM APO for 72 h by means of an anti-PML antibody (PM001; MBL) that can recognize most of the PML splicing variants and is useful for immunofluorescence analysis. The results showed that PML was localized predominantly in punctate nuclear speckles termed PML-NBs in control O cells (Fig. 4A). Interestingly, we noticed that some nuclear PML, but not all, disappeared and was translocated into discrete cytoplasmic bodies in the O cells treated with 1 μM ATO (Fig. 4A). We also observed cytoplasmic translocation of PML in the O cells treated with 1 μM APO for 72 h (Fig. 4A). Furthermore, we observed a similar cytoplasmic translocation of PML in the HCV-negative 293FT or HeLa

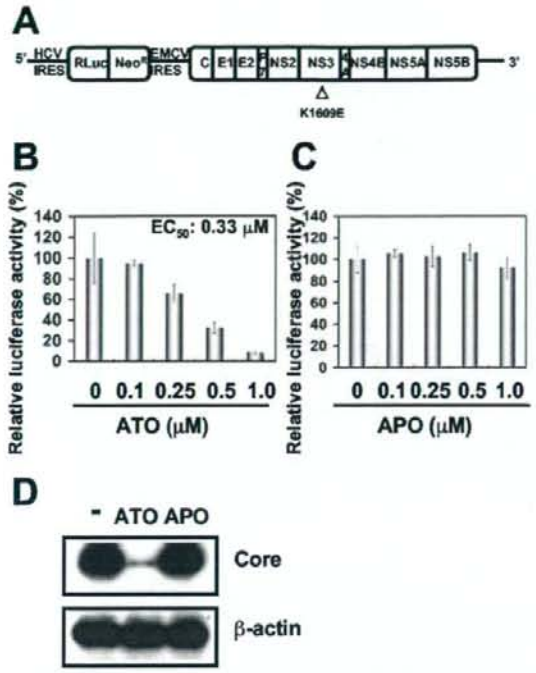

FIG. 2. Effect of APO on HCV replication. (A) Schematic representation of genome-length HCV RNA encoding the RL gene as a reporter (ORN/C-5B/KE RNA) replicated in OR6 cells. The RL is expressed as a fusion protein with neomycin phosphotransferase (Neo^R). The position of an adaptive mutation, K1609E in NS3, is indicated by an open triangle. (B) Effect of ATO on genome-length HCV RNA replication. At 72 h after treatment of OR6 cells with ATO at the indicated concentrations, the replication level of HCV RNA was monitored by the RL assay. The relative RL activity is shown. The results shown are means from three independent experiments. Error bars indicate standard deviations. (C) Effect of APO on genome-length HCV RNA replication. At 72 h after treatment of OR6 cells with APO at the indicated concentrations, the replication level of HCV RNA was monitored by the RL assay as described for panel B. (D) HCV core protein expression level in O cells after treatment with either ATO or APO. The results of Western blot analysis of cellular lysates with anti-HCV core or anti-β-actin antibody in O cells at 72 h after treatment with either 1 μM ATO or 1 μM APO are shown.

cells after the treatment with ATO (data not shown). Thus, we concluded that the cytoplasmic translocation of PML after the treatment with ATO was not associated with anti-HCV activity. Next, Western blot analysis to compare PML expression in the lysates of O cells treated with 1 μM ATO or 1 μM APO for 72 h was performed using another anti-PML antibody, A301-168A-1 (a gift from Bethyl Laboratories), which can recognize the longest isoform, PML I, but not shorter PML isoforms such as PML VI and which has been proven useful for Western blot analysis. Consistent with the previous finding that ATO promotes PML degradation (70), the expression level of the PML I protein was lower in the ATO-treated O cells than in the APO-treated O cells (Fig. 4B), suggesting that PML degradation by ATO is associated with anti-HCV activity. To further examine whether PML is directly involved in the anti-HCV activity of ATO, we used lentiviral vector-mediated RNA interference to stably knock down PML in the O cells. To express an shRNA targeted to all PML isoforms (56), we used the VSV G-pseudotyped HIV-1-based vector system (1, 42, 71). We used the puromycin-resistant pooled cells at 10 days after the lentiviral transduction in this experiment. Immunofluorescence and Western blot analysis demonstrated a very effective knockdown of PML in the O cells (Fig. 4C and D). We quantitatively examined the level of HCV RNA in the PML knockdown O cells treated with or without either 1 μM ATO (Fig. 4E) or 1 μM APO (Fig. 4F) for 72 h. The results showed that the replication level of genome-length HCV-O RNA in the untreated PML knockdown cells was similar to that in control cells (Fig. 4E), suggesting that PML is dispensable in HCV RNA replication. Importantly, ATO effectively inhibited the HCV RNA replication in both the PML knockdown cells and control cells compared with that of the APO-treated cells (Fig. 4E and F). Thus, we concluded that PML was dispensable for the anti-HCV activity of ATO. Since the Chk2 checkpoint kinase has recently been implicated in ATO-induced apoptosis and in association with PML (27, 63, 64, 66), we examined the anti-HCV activity in the ATO-treated Chk2 knockdown O cells (3). As we previously described, Western blot analysis demonstrated very effective knockdown of Chk2 in O cells (Fig. 4G). Accordingly, we examined the level of HCV RNA in Chk2 knockdown cells treated with or without either 1 μM ATO (Fig. 4H) or 1 μM APO (Fig. 4I) for 72 h. Consistent with our recent finding that Chk2 is required for HCV RNA replication, the replication of genome-length HCV RNA in the untreated Chk2 knockdown cells was remarkably suppressed (Fig. 4H). However, ATO strongly inhibited the HCV RNA replication in the Chk2 knockdown cells compared with that in the APO-treated Chk2 knockdown cells (Fig. 4H and I), suggesting that Chk2 is not implicated in the anti-HCV activity of ATO.

Effect of ATO on the stress-signaling pathways. To date, the focus has been on PML and PML-retinoic acid receptor α as major targets of ATO (70). On the other hand, arsenic has been reported to modulate other cell-signaling pathways, especially stress-responsive transcription factors, such as nuclear factor κB (NF-κB), activator protein 1 (AP-1), and STAT3 (12, 37, 38, 62). Therefore, we examined the involvement of several stress-responsive pathways in the anti-HCV activity of ATO by luciferase-based reporter assays or Western blot analysis using an antibody which specifically recognizes STAT3 phosphorylated at tyrosine 705. Although it has been reported that ATO inhibited the NF-κB signaling pathway through a direct interaction with IKKβ at a high concentration (more than 10 μM) (29), neither 1 μM ATO nor 1 μM APO affected the endogenous NF-κB transcriptional activity in the present study (Fig. 5A and B). Conversely, ATO at least slightly stimulated mitogen-activated protein kinase kinase kinase (MEKK)-mediated NF-κB activation (Fig. 5A and B). Since NF-κB activation has been shown to stimulate HCV replication (60), the NF-κB pathway would seem not to be essential for the anti-HCV activity of ATO. Next, regarding the AP-1 signaling pathway, both ATO and APO are known to activate c-Jun N-terminal kinase (JNK) (45). Importantly, there was no stimulation of JNK activity at a dose below 30 μM (45). In fact, 50 μM ATO but not 50 μM APO strongly stimulates AP-1 activity by in-

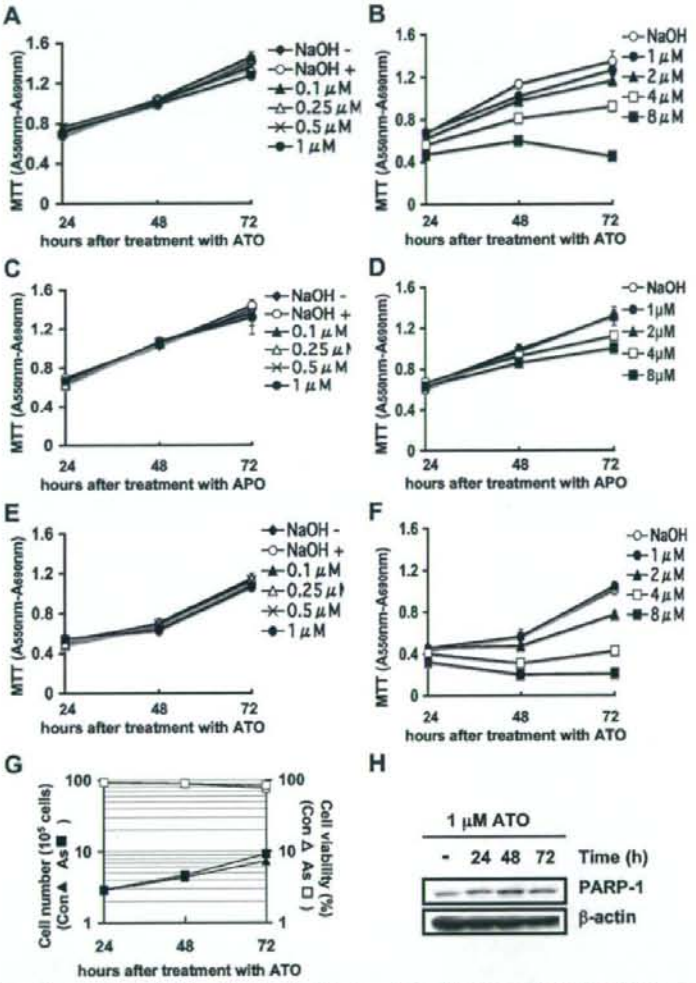

FIG. 3. Effect of ATO on cell growth and viability. (A and B) MTT assay of O cell lysates at the indicated times after treatment with ATO at various concentrations. NaOH (10 μM) was used as the solvent for ATO. The results shown are means from three independent experiments. Error bars indicate standard deviations. (C and D) MTT assay of O cell lysates at the indicated times after treatment with APO at various concentrations. (E and F) MTT assay of HuH-7 cell lysates at the indicated times after treatment with ATO at various concentrations. (G) Growth curve and viability of O cells after treatment with either 10 μM NaOH (Con) or 1 μM ATO (As). (H) Western blot analysis of cellular lysates with anti-PARP-1 or anti-β-actin antibody in O cells at the indicated times after treatment with 1 μM ATO.

hibiting a JNK phosphatase (10). Consistently, we found that both 1 μM ATO and 1 μM APO had a marginal effect on the AP-1 signaling pathway (Fig. 5C and D), suggesting that the AP-1 pathway is also not involved in the anti-HCV activity of ATO. Regarding the STAT3 signaling pathway, ATO has been reported to inhibit the phosphorylation of the STAT3 tyrosine at 705, leading to inactivation of the JAK-STAT signaling pathway (12, 62). In contrast, it has been reported that HCV constitutively phosphorylates and activates STAT3 (49, 59, 67). In this context, we observed constitutive tyrosine phosphorylation of STAT3 in untreated O cells (Fig. 5E). Furthermore, the marginal effect of 1 μM ATO on STAT3 phosphorylation and interleukin-6-mediated STAT3 activation was also observed (Fig. 5E and F). Taken together, these results at least suggest that the NF-κB, AP-1, and STAT3 pathways may not be associated with the anti-HCV activity of ATO at submicromolar concentrations.

The anti-HCV activity of ATO is associated with the glutathione redox system and oxidative stress. Finally, we focused on the involvement of the glutathione redox system and oxidative stress in the anti-HCV activity of ATO. For this, we analyzed the HCV replication level after combination treatment with ATO and antioxidants such as NAC and vitamin C using the OR6 assay system. When OR6 cells were treated with

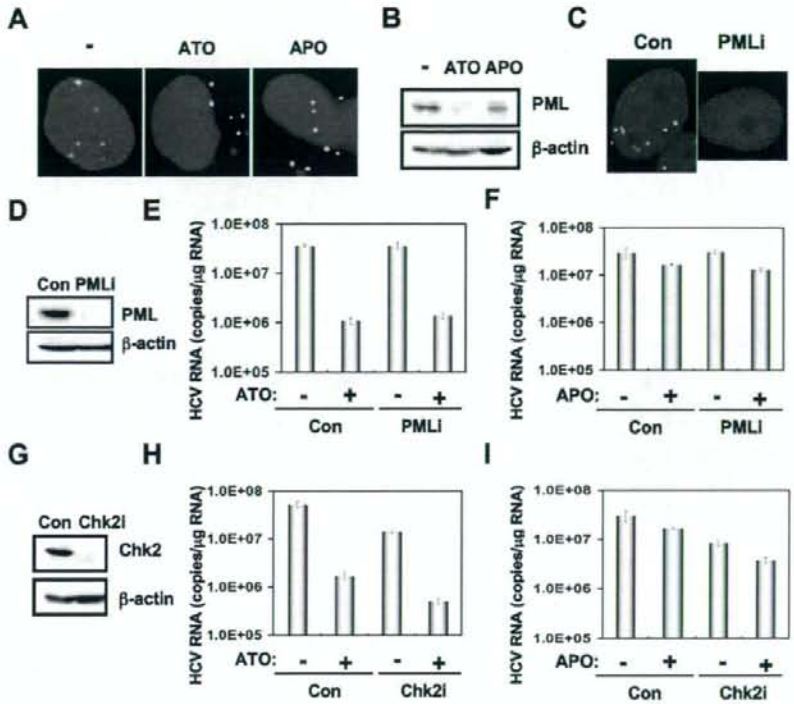

FIG. 4. PML and Chk2 are not required for the anti-HCV activity of ATO. (A) Subcellular localization of PML in O cells at 72 h after treatment with 10 μM NaOH (−), 1 μM ATO, or 1 μM APO. PML was detected by indirect immunofluorescence analysis with anti-PML antibody (PM001). DAPI staining of the nuclear DNA is also shown. (B) Induction of PML degradation by ATO but not by APO. The results of Western blot analysis of cellular lysates of O cells at 72 h after treatment with 10 μM NaOH (−), 1 μM ATO, or 1 μM APO with anti-PML (A301-168A-1) or anti-β-actin antibody are shown. (C) Stable knockdown of PML by shRNA-producing lentiviral vector in O cells. PML was detected by indirect immunofluorescence analysis with anti-PML antibody (PM001) in O cells expressing shRNA targeted to PML (PMLi) as well as in O cells transduced with a control lentiviral vector (Con). (D) Western blot analysis of cellular lysates with anti-PML (A301-168A-1) or anti-β-actin antibody in PML knockdown O cells (PMLi) as well as in control O cells (Con). (E and F) The level of genome-length HCV-O RNA was monitored by real-time LightCycler PCR in PML knockdown O cells (PMLi) as well as in control O cells (Con) after treatment with 10 μM NaOH (−), 1 μM ATO (+) (E), or 1 μM APO (+) (F) for 72 h. Results from three independent experiments conducted as described in the legend to Fig. 1A are shown. (G) Inhibition of Chk2 expression by shRNA-producing lentiviral vector. The results of Western blot analysis of cellular lysates with anti-Chk2 or anti-β-actin antibody in O cells expressing shRNA targeted to Chk2 (Chk2i) as well as in O cells transduced with a control lentiviral vector (Con) are shown. (H and I) The level of genome-length HCV-O RNA was monitored by real-time LightCycler PCR in Chk2 knockdown O cells (Chk2i) as well as in control O cells (Con) after treatment with 10 μM NaOH (−), 1 μM ATO (+) (H), or 1 μM APO (+) (I) for 72 h. Results from three independent experiments conducted as described in the legend to Fig. 1A are shown.

either 100 μM vitamin C or 10 mM NAC alone for 24 h or 72 h, the HCV replication was slightly enhanced (Fig. 6A and B), indicating that the antioxidant can activate HCV replication. Although the anti-HCV activity in the OR6 cells treated with 1 μM ATO and in combination with 100 μM vitamin C for 24 h was weakly reduced, 10 mM NAC completely and partially eliminated the anti-HCV activity of ATO after 24 h (Fig. 6A) and 72 h (Fig. 6B) of treatment, respectively, suggesting that oxidative stress and the glutathione redox system are associated with the anti-HCV activity of ATO. In contrast, the iNOS inhibitor 1400W did not suppress the HCV RNA replication or eliminate the anti-HCV activity of ATO, suggesting that NO is not involved in the anti-HCV activity of ATO (Fig. 6C). To further examine the involvement of oxidative stress in the anti-HCV activity of ATO, we examined ROS production in ATO-treated cells using two oxidative-sensitive fluorescent probes, DHE for detection of intracellular O_2^- and DCF for detection of intracellular H_2O_2. We found that 1 μM ATO could generate a significant level of intracellular O_2^- but not intracellular H_2O_2, while 2 μM BSO, an inhibitor of glutathione synthesis (14, 20, 33), could induce both O_2^- and H_2O_2 (Fig. 6D to H). Importantly, NAC diminished the ATO-dependent O_2^- induction (Fig. 6F). Since glutathione is a major antioxidant in cells and can clear away superoxide anion free radical, we also analyzed the changes of the intracellular glutathione level in ATO-treated O cells using CMF fluorescence, which can react with glutathione. As a result, we observed significant glutathione depletion in the cells treated with at least 1 μM ATO (Fig. 6I). To further confirm the involvement of glutathione in the anti-HCV activity of ATO, we examined the effect of cotreatment with ATO and BSO. When the OR6 cells were treated with 1 μM BSO alone, the HCV replication

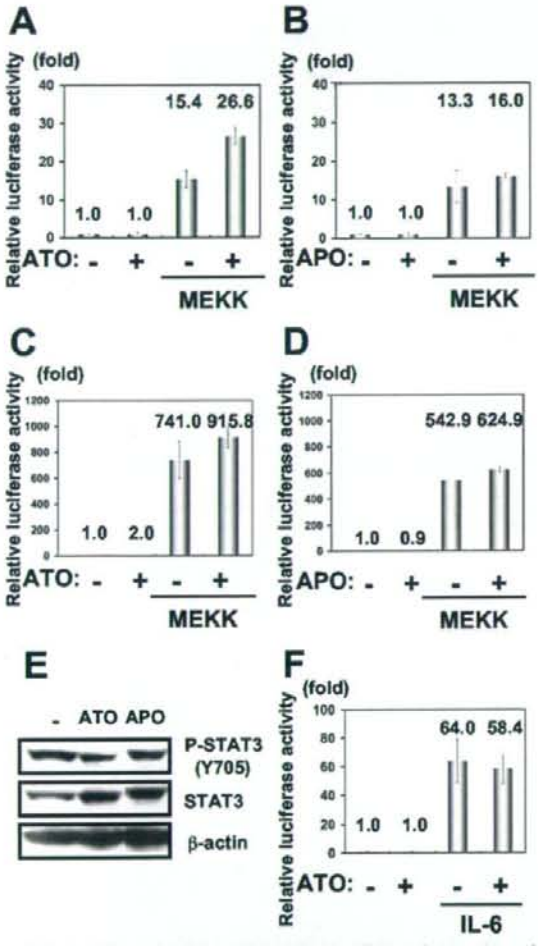

FIG. 5. Effect of ATO on the stress-signaling pathways. (A and B) Effect of ATO or APO on the NF-κB signaling pathway. O cells were transfected with 100 ng of reporter plasmid, pNF-κB-Luc, and/or 100 ng of pFC-MEKK (Stratagene, La Jolla, CA). Cells were treated with either 1 μM ATO (A) or 1 μM APO (B), and an FL assay was performed 24 h later. The results shown are means from three independent experiments. The relative FL activity is shown. (C and D) Effect of ATO or APO on the AP-1 signaling pathway. O cells were transfected with 100 ng of pAP-1-Luc and/or 100 ng of pFC-MEKK (Stratagene). Cells were treated with either 1 μM ATO (C) or 1 μM APO (D), and an FL assay was performed 24 h later as described for panels A and B. (E) Effect of ATO on the phosphorylation level of STAT3 at tyrosine 705. The results of Western blot analysis of cellular lysates with anti-phospho-STAT3 (Tyr705), anti-STAT3, or anti-β-actin antibody in O cells treated with either 1 μM ATO or 1 μM APO for 24 h are shown. (F) Effect of ATO on the STAT3 signaling pathway. O cells were transfected with 100 ng of STAT3 reporter APRE-Luc (41) (STAT3-Luc, a generous gift from T. Hirano, Osaka University, Japan). Cells were treated with 1 μM ATO for 19 h and then stimulated with 100 ng/ml of interleukin-6 for 5 h, and an FL assay was performed as described for panels A and B.

level was suppressed by about 30% compared with that of the control cells, and this occurred without cell toxicity (data not shown). However, consistent with previous reports in which ATO-induced apoptosis was enhanced by BSO (14, 20, 33), most of the cells died, possibly through apoptosis, when the OR6 cells were cotreated with 1 μM ATO and 1 μM BSO for 72 h (data not shown), suggesting that ATO and BSO synergistically generate ROS and deplete glutathione, resulting in induction of oxidative damage. Taken together, these results suggest that ATO may inhibit the HCV RNA replication by modulating the glutathione redox system and oxidative stress.

DISCUSSION

ATO has been reported to affect multiple biological functions, such as PML-NB formation, apoptosis, differentiation, stress response, and viral infection (38). Indeed, ATO has been shown to increase retroviral infectivity, including infectivity of HIV-1, HIV-2, feline immunodeficiency virus, simian immunodeficiency virus from rhesus macaques, and murine leukemia virus, although the mechanisms responsible for these changes are not well understood (5, 6, 32, 44, 47, 50, 57). PML, which is involved in host antiviral defenses, is required for the formation of the PML-NB, which is often disrupted or sequestered in the cytoplasm by infection with DNA or RNA viruses (17). The fact that ATO promotes the degradation of PML and alters the morphology or distribution of PML-NBs suggests that ATO enhances HIV-1 infection by antagonizing an antiviral activity associated with PML. In fact, HIV-1 infection has been reported to alter PML localization (57), although others have failed to confirm this finding (5). Furthermore, Berthoux et al. demonstrated that ATO stimulated retroviral reverse transcription (5). Moreover, ATO has been shown to have an inhibitory effect on host restriction factors, such as TRIM5a, Refl, and Lv1, in a cell type-dependent manner (5, 6, 32, 44, 47, 50). In contrast, we have demonstrated that ATO strongly inhibited genome-length HCV RNA replication without cell toxicity (Fig. 1A and 2A). In addition, we observed the cytoplasmic translocation of PML in the HCV RNA-replicating O cells after the treatment with ATO (Fig. 4A). However, PML was dispensable for the anti-HCV activity of ATO as well as HCV RNA replication (Fig. 4E). In this regard, it is worth noting the recent report by Herzer et al. that the HCV core protein interacts with PML isoform IV and abrogates the PML function (22). Thus, PML may be involved in the HCV life cycle. In any case, the sensitivity to ATO and the cellular target of ATO seem to be different between HCV and HIV-1.

HCV infection has been shown to cause a state of chronic oxidative stress like that seen in chronic hepatitis C, which may contribute to fibrosis and carcinogenesis in the liver (16, 18, 40). In particular, HCV replication has been associated with the endoplasmic reticulum (ER), where HCV causes ER stress. Indeed, HCV NS5A and core, the ER-associated proteins, have been reported to trigger ER stress (4, 55). Therefore, HCV infection causes production of ROS and lowering of mitochondrial transmembrane potential through calcium signaling (4, 36). Among the HCV proteins, core, E1, NS3, and NS5A have been shown to be potent ROS inducers, and these HCV proteins also alter intracellular calcium levels and induce oxidative stress, thereby inducing DNA damage, and constitu-

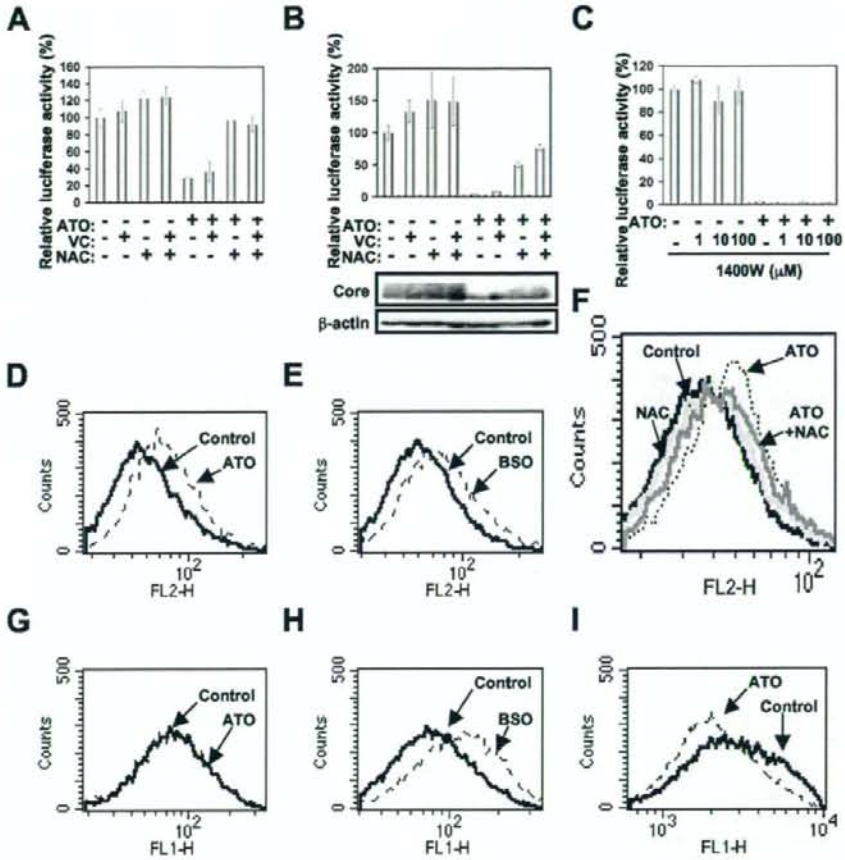

FIG. 6. The anti-HCV activity of ATO is associated with the glutathione redox system and oxidative stress. (A and B) The anti-HCV activity of ATO is eliminated by treatment with the antioxidant NAC. OR6 cells were treated with 1 μM ATO alone and in combination with 100 μM vitamin C (VC), with or without 10 mM NAC, for 24 h (A) or 72 h (B). The replication level of HCV RNA was monitored by the RL assay. The relative RL activity is shown. The results shown are means from three independent experiments; error bars indicate standard deviations. The results of Western blot analysis of cellular lysates with anti-HCV core or anti-β-actin antibody in OR6 cells at 72 h after the treatment with 1 μM ATO alone and in combination with 100 μM VC, with or without 10 mM NAC, are also shown. (C) Effect of combination treatment with ATO and the iNOS inhibitor 1400W on HCV RNA replication. OR6 cells were treated with 1 μM ATO alone and in combination with 1400W at the indicated concentrations for 72 h. The replication level of HCV RNA was monitored by the RL assay as described for panels A and B. (D and E) Effect of ATO on production of a ROS, O_2^-, in O cells. O cells were treated with 1 μM ATO (D) or 2 μM BSO (E) for 24 h. The intracellular O_2^- level was measured by flow cytometry using DHE as described in Materials and Methods. (F) Inhibition of ATO-dependent O_2^- induction by NAC. O cells were treated with either 1 μM ATO or 10 mM NAC alone and in combination with 10 mM NAC for 24 h. (G and H) Effect of ATO on production of a ROS, H_2O_2, in O cells. O cells were treated with 1 μM ATO (G) or 2 μM BSO (H) for 24 h. The intracellular H_2O_2 level was measured by flow cytometry using DCF as described in Materials and Methods. (I) Effect of ATO on the intracellular glutathione level in O cells. O cells were treated with 1 μM ATO for 72 h. The intracellular glutathione level was measured by flow cytometry using CellTracker Green CMFDA as described in Materials and Methods.

tively activate STAT3 and NF-κB, which are associated with HCV pathogenesis (19, 34, 36, 43, 49, 59, 60, 67). In fact, oxidative stress has been shown to trigger STAT3 tyrosine phosphorylation and nuclear translocation, which correlate with the activation of STAT3, leading to its DNA-binding activity (9). In contrast, ATO inhibited the STAT3 tyrosine phosphorylation through direct interaction with JAK kinase, thereby suppressing the transcriptional activity of STAT3 (12, 62). Importantly, STAT3 activation has been reported to be associated with HCV RNA replication (59, 69). The STAT3 Tyr705 dominant negative mutant has been shown to inhibit HCV RNA replication, suggesting that STAT3 positively regulates HCV replication (59). In contrast, others have reported that STAT3 induces anti-HCV activity (69). In this study, we analyzed the potential effect of ATO treatment on a set of stress-signaling events, including the NF-κB, AP-1, and STAT3 pathways, since ATO is known to modulate various signaling pathways. However, at 1 μM, which exerted an anti-HCV activity, the respective signaling pathways were not affected, arguing that the anti-HCV activity is independent of these

pathways (Fig. 5). In this regard, these stress-signaling pathways have been reported to be constitutively activated in HCV core- or NS5A-expressing cells (19, 36, 49, 59, 60, 67). In addition, previous studies demonstrated that ATO modulates the NF-κB, AP-1, and STAT3 pathways at higher concentrations (NF-κB, >10 μM; AP-1, >30 μM; STAT3, >4 μM). Therefore, we may have only observed the marginal effect of ATO in this study (Fig. 5). On the other hand, the HCV core or NS3 protein as well as HCV infection induces NO, leading to induction of double-stranded DNA breaks and accumulation of mutations of cellular genes (35). However, the iNOS inhibitor 1400W could not suppress HCV RNA replication and the anti-HCV activity of ATO, indicating that NO is not associated with the anti-HCV activity or with HCV replication (Fig. 6C).

It has been indicated that oxidative damage plays an important role in the effect of ATO (38). ROS generated in response to ATO exposure lead to accumulation of intracellular H_2O_2. Glutathione peroxidase and catalase are key enzymes regulating the levels of ROS and protecting cells from ATO-induced damage (26). However, the gastrointestinal glutathione peroxidase was drastically downregulated in cells harboring HCV replicons, which are rendered more susceptible to oxidative stress (39). The glutathione redox system has been implicated in the cellular defense system (14, 20). Glutathione, a major antioxidant in cells, is a tripeptide synthesized from cysteine, glutamic acid, and glycine, and it can scavenge superoxide anion free radicals. ATO has been shown to bind to the sulfhydryl group of glutathione and deplete the intracellular glutathione, resulting in enhancement of the sensitivity to oxidative damage (20, 33). Conversely, the antioxidant NAC is readily taken up by cells and serves as a precursor to elevate intracellular glutathione (53). In fact, ATO-induced apoptosis has been shown to be inhibited by NAC (11, 14, 21, 28). In this study, we have demonstrated that the anti-HCV activity of ATO was completely eliminated by treatment with NAC for 24 h (Fig. 6A). In addition, we found that ATO increased intracellular O_2^- but not H_2O_2 and depleted the intracellular glutathione in HCV RNA-replicating cells (Fig. 6D to I). Importantly, NAC diminished the ATO-dependent O_2^- induction (Fig. 6F). This finding could strengthen the link between ATO-dependent oxidative stress and anti-HCV activity. Similarly, Wen et al. reported an increase in ROS and enhanced susceptibility to glutathione depletion in the HCV core-expressing HepG2 cells (61). Accordingly, ROS have been shown to significantly suppress RNA replication in HCV replicon-harboring cells treated with H_2O_2 (13). In addition, HCV replication has been shown to be inhibited by lipid peroxidation of arachidonate, and this peroxidation could be blocked by lipid-soluble antioxidants such as vitamin E (23). Conversely, several antioxidants, such as vitamin C, vitamin E, and NAC, enhanced HCV replication in the present study (Fig. 6A and B) (65). Thus, we suggest that ATO inhibited HCV RNA replication by modulating the glutathione redox system and oxidative stress. In contrast to the above findings with HCV, NAC has been shown to suppress HIV-1 replication by preventing the activation of HIV-1 long terminal repeat transcription by NF-κB, suggesting a correlation between a decrease in glutathione levels and activation of HIV-1 replication (46, 53, 54). In this context, ATO has shown opposite effects on HIV-1 and HCV replication, stimulating the former and inhibiting the latter. Considering all of these results together, ATO can be regarded as a useful, novel anti-HCV reagent. In addition, the host redox system may be critical for HCV replication and may represent a pivotal target for the clinical treatment of patients with chronic hepatitis C.

ACKNOWLEDGMENTS

We thank D. Trono, R. Agami, R. Iggo, A. Takamizawa, T. Hirano, A. Yoshimura, and M. Hijikata for the VSV G-pseudotyped HIV-1-based vector system pCMVΔR8.91, pMDG2, pSUPER, pRDI292, anti-NS5A antibody, APRE-Luc, and 293FT cells. We also thank T. Stamminger, M. Yano, and T. Nakamura for their helpful suggestions and technical assistance.

This work was supported by a Grant-in-Aid for Scientific Research (C) from the Japan Society for the Promotion of Science (JSPS); by a Grant-in-Aid for Research on Hepatitis from the Ministry of Health, Labor, and Welfare of Japan; by the Kawasaki Foundation for Medical Science and Medical Welfare; by the Okayama Medical Foundation; and by the Ryobi Teien Memorial Foundation.

REFERENCES

1. **Ariumi, Y., T. Priscilla, M. Masutani, and D. Trono.** 2005. DNA damage sensors ATM, ATR, DNA-PKcs, and PARP-1 are dispensable for human immunodeficiency virus type 1 integration. J. Virol. **79:**2973–2978.
2. **Ariumi, Y., M. Kuroki, K. Abe, H. Dansako, M. Ikeda, T. Wakita, and N. Kato.** 2007. DDX3 DEAD-box RNA helicase is required for hepatitis C virus RNA replication. J. Virol. **81:**13922–13926.
3. **Ariumi, Y., M. Kuroki, H. Dansako, K. Abe, M. Ikeda, T. Wakita, and N. Kato.** 2008. The DNA damage sensors, ataxia-telangiectasia mutated kinase and checkpoint kinase 2 are required for hepatitis C virus RNA replication. J. Virol. **82:**9639–9646.
4. **Benali-Furet, N. L., M. Chami, L. Houel, F. De Giorgi, F. Vernejoul, D. Lagorce, L. Buscail, R. Bartenschlager, F. Ichas, R. Rizzuto, and P. Paterlini-Bréchot.** 2005. Hepatitis C virus core triggers apoptosis in liver cells by inducing ER stress and ER calcium depletion. Oncogene **24:**4921–4933.
5. **Berthoux, L., G. J. Towers, C. Gurer, P. Salomoni, P. P. Pandolfi, and J. Luban.** 2003. As2O3 enhances retroviral reverse transcription and counteracts Ref1 antiviral activity. J. Virol. **77:**3167–3180.
6. **Berthoux, L., S. Sebastian, E. Sokolskaja, and J. Luban.** 2004. Lv1 inhibition of human immunodeficiency virus type 1 is counteracted by factors that stimulate synthesis or nuclear translocation of viral cDNA. J. Virol. **78:**11739–11750.
7. **Bridge, A. J., S. Pebernard, A. Ducraux, A. L. Nicoulaz, and R. Iggo.** 2003. Induction of an interferon response by RNAi vectors in mammalian cells. Nat. Genet. **34:**263–264.
8. **Brummelkamp, T. R., R. Bernard, and R. Agami.** 2002. A system for stable expression of short interfering RNAs in mammalian cells. Science **296:**550–553.
9. **Carballo, M., M. Conde, R. E. Bekay, J. Martín-Nieto, M. J. Camacho, J. Monteseirín, J. Conde, F. J. Bedoya, and F. Sobrino.** 1999. Oxidative stress triggers STAT3 tyrosine phosphorylation and nuclear translocation in human lymphocytes. J. Biol. Chem. **274:**17580–17586.
10. **Cavigelli, M., W. W. Li, A. Lin, B. Su, K. Yoshioka, and M. Karin.** 1996. The tumor promoter arsenite stimulates AP-1 activity by inhibiting a JNK phosphatase. EMBO J. **15:**6269–6279.
11. **Chen, Y. C., S. Y. Lin-Shiau, and J. K. Lin.** 1998. Involvement of reactive oxygen species and caspase 3 activation in arsenite-induced apoptosis. J. Cell Physiol. **177:**324–333.
12. **Cheng, H. Y., P. Li, M. David, T. E. Smithgall, L. Feng, and M. W. Lieberman.** 2004. Arsenic inhibition of the JAK-STAT pathway. Oncogene **23:**3603–3612.
13. **Choi, J., K. J. Lee, Y. Zheng, A. K. Yamaga, M. M. C. Lai, and J. H. Ou.** 2004. Reactive oxygen species suppress hepatitis C virus RNA replication in human hepatoma cells. Hepatology **39:**81–89.
14. **Dai, J., R. S. Weinberg, S. Waxman, and Y. Jing.** 1999. Malignant cells can be sensitized to undergo growth inhibition and apoptosis by arsenic trioxide through modulation of the glutathione redox system. Blood **93:**268–277.
15. **Davis, G. L.** 2006. Tailoring antiviral therapy in hepatitis C. Hepatology **43:**909–911.
16. **De Maria, N., A. Colantoni, S. Fagiuoli, G. J. Liu, B. K. Rogers, F. Farinati, D. H. Van Thiel, and R. A. Floyd.** 1996. Association between reactive oxygen species and disease activity in chronic hepatitis C. Free Radic. Biol. Med. **21:**291–295.
17. **Everett, R. D., and M. K. Chelbi-Alix.** 2007. PML and PML nuclear bodies: implications in antiviral defence. Biochemie **89:**819–830.
18. **Farinati, F., R. Cardin, N. De Maria, G. D. Libera, C. Marafin, E. Lecis, P.**

Burra, A. Floreani, A. Cecchetto, and R. Naccarato. 1995. Iron storage, lipid peroxidation and glutathione turnover in chronic anti-HCV positive hepatitis. J. Hepatol. **22:**449–456.
19. **Gong, G., G. Waris, R. Tanveer, and A. Siddiqui.** 2001. Human hepatitis C virus NS5A protein alters intracellular calcium levels, induces oxidative stress, and activates STAT-3 and NF-κB. Proc. Natl. Acad. Sci. USA **98:** 9599–9604.
20. **Han, Y. H., S. H. Kim, S. Z. Kim, and W. H. Park.** 2008. Apoptosis in arsenic trioxide-treated Calu-6 lung cells is correlated with the depletion of GSH levels rather than the change of ROS levels. J. Cell. Biochem. **104:**862–878.
21. **Han, Y. H., S. Z. Kim, S. H. Kim, and W. H. Park.** 2008. Suppression of arsenic trioxide-induced apoptosis in HeLa cells by N-acetylcysteine. Molecules Cells **26:**18–25.
22. **Herzer, K., S. Weyer, P. H. Krammer, P. R. Galle, and T. G. Hofmann.** 2005. Hepatitis C virus core protein inhibits tumor suppressor protein promyelocytic leukemia function in human hepatoma cells. Cancer Res. **65:**10830–10837.
23. **Huang, H., Y. Chen, and J. Ye.** 2007. Inhibition of hepatitis C virus replication by peroxidation of arachidonate and restoration by vitamin E. Proc. Natl. Acad. Sci. USA **104:**18666–18670.
24. **Hwang, D. R., Y. C. Tsai, J. C. Lee, K. K. Huang, R. K. Lin, C. H. Ho, J. M. Chiou, Y. T. Lin, J. T. A. Hsu, and C. T. Yeh.** 2004. Inhibition of hepatitis C virus replication by arsenic trioxide. Antimicrob. Agents Chemother. **48:** 2876–2882.
25. **Ikeda, M., K. Abe, H. Dansako, T. Nakamura, K. Naka, and N. Kato.** 2005. Efficient replication of a full-length hepatitis C virus genome, strain O, in cell culture, and development of a luciferase reporter system. Biochem. Biophys. Res. Commun. **329:**1350–1359.
26. **Jing, Y., J. Dai, R. M. E. Chalmers-Redman, W. G. Tatton, and S. Waxman.** 1999. Arsenic trioxide selectively induces acute promyelocytic leukemia cell apoptosis via a hydrogen peroxide-depndent pathway. Blood **94:**2102–2111.
27. **Joe, Y., J. H. Jeong, S. Yang, H. Kang, N. Motoyama, P. P. Pandolfi, J. H. Chung, and M. K. Kim.** 2006. ATR, PML, and Chk2 play a role in arsenic trioxide-induced apoptosis. J. Biol. Chem. **281:**28764–28771.
28. **Kang, Y. H., M. J. Yi, M. J. Kim, M. T. Park, S. Bae, C. M. Kang, C. K. Cho, I. C. Park, M. J. Park, C. H. Rhee, S. I. Hong, H. Y. Chung, Y. S. Lee, and S. J. Lee.** 2004. Caspase-independent cell death by arsenic trioxide in human cervical cancer cells: reactive oxygen species-mediated poly(ADP-ribose) polymerase-1 activation signals apoptosis-inducing factor release from mitochondria. Cancer Res. **64:**8960–8967.
29. **Kapahi, P., T. Takahashi, G. Natoli, S. R. Adams, Y. Chen, R. Y. Tsien, and M. Karin.** 2000. Inhibition of NF-κB activation by arsenite through reaction with a critical cysteine in the activation loop of IκB kinase. J. Biol. Chem. **275:**36062–36066.
30. **Kato, N.** 2001. Molecular virology of hepatitis C virus. Acta Med. Okayama **55:**133–159.
31. **Kato, N., K. Sugiyama, K. Namba, H. Dansako, T. Nakamura, M. Takami, K. Naka, A. Nozaki, and K. Shimotohno.** 2003. Establishment of a hepatitis C virus subgenomic replicon derived from human hepatocytes infected in vitro. Biochem. Biophys. Res. Commun. **306:**756–766.
32. **Keckesova, Z., L. M. J. Ylinen, and G. J. Towers.** 2004. The human and African green monkey TRIM5α genes encode Ref1 and Lv1 retroviral restriction factor activities. Proc. Natl. Acad. Sci. USA **101:**10780–10785.
33. **Kito, M., Y. Akao, N. Ohishi, K. Yagi, and Y. Nozawa.** 2002. Arsenic trioxide-induced apoptosis and its enhancement by buthionine sulfoximine in hepatocellular carcinoma cell lines. Biochem. Biophys. Res. Commun. **291:**861–867.
34. **Korenaga, M., T. Wang, Y. Li, L. A. Showalter, T. Chan, J. Sun, and S. A. Weinman.** 2005. Hepatitis C virus core protein inhibits mitochondrial electron transport and increases reactive oxygen species (ROS) production. J. Biol. Chem. **280:**37481–37488.
35. **Machida, K., K. T. Cheng, V. M. Sung, K. J. Lee, A. M. Levine, and M. M. C. Lai.** 2004. Hepatitis C virus infection activates the immunologic (type II) isoform of nitric oxide synthase and thereby enhances DNA damage and mutations of cellular genes. J. Virol. **78:**8835–8843.
36. **Machida, K., K. T. H. Cheng, C. K. Lai, K. S. Jeng, V. M. H. Sung, and M. M. C. Lai.** 2006. Hepatitis C virus triggers mitochondrial permeability transition with production of ractive oxygen species, leading to DNA damage and STAT3 activation. J. Virol. **80:**7199–7207.
37. **Meyer, M., R. Schreck, and P. A. Baeuerle.** 1993. H_2O_2 and antioxidants have opposite effects on activation of NF-κB and AP-1 in intact cells: AP-1 as secondary antioxidant-responsive factor. EMBO J. **12:**2005–2015.
38. **Miller, W. H., Jr., H. M. Schipper, J. S. Lee, J. Singer, and S. Waxman.** 2002. Mechanisms of action of arsenic trioxide. Cancer Res. **62:**3893–3903.
39. **Morbitzer, M., and T. Herget.** 2005. Expression of gastrointestinal glutathione peroxidase is inversely correlated to the presence of hepatitis C virus subgenomic RNA in human liver cells. J. Biol. Chem. **280:**8831–8841.
40. **Moriya, K., K. Nakagawa, T. Santa, Y. Shintani, H. Fujie, H. Miyoshi, T. Tsutsumi, T. Miyazawa, K. Ishibashi, T. Horie, K. Imai, T. Todoroki, S. Kimura, and K. Koike.** 2001. Oxidative stress in the absence of inflammation in a mouse model for hepatitis C virus-associated hepatocarcinogenesis. Cancer Res. **61:**4365–4370.
41. **Nakajima, K., Y. Yamanaka, K. Nakae, H. Kojima, M. Ichiba, N. Kiuchi, T. Kitaoka, T. Fukada, M. Hibi, and T. Hirano.** 1996. A central role for STAT3 in IL-6-induced regulation of growth and differentiation in M1 leukemia cells. EMBO J. **15:**3651–3658.
42. **Naldini, L., U. Blömer, P. Gallay, D. Ory, R. Mulligan, F. H. Gage, I. M. Verma, and D. Trono.** 1996. In vivo gene delivery and stable transduction of nondividing cells by a lentiviral vector. Science **272:**263–267.
43. **Okuda, M., K. Li, M. R. Beard, L. A. Showalter, F. Scholle, S. M. Lemon, and S. A. Weinman.** 2002. Mitochondrial injury, oxidative stress, and antioxidant gene expression are induced by hepatitis C virus core protein. Gastroenterology **122:**366–375.
44. **Pion, M., R. Stalder, R. Correa, B. Mangeat, G. J. Towers, and V. Piguet.** 2007. Identification of an arsenic-sensitive block to primate lentiviral infection of human dendritic cells. J. Virol. **81:**12086–12090.
45. **Porter, A. C., G. R. Fanger, and R. R. Vaillancourt.** 1999. Signal transduction pathways regulated by arsenate and arsenite. Oncogene **18:**7794–7802.
46. **Roederer, M., F. J. T. Staal, P. A. Raju, S. W. Ela, L. A. Herzenberg, and L. A. Herzenberg.** 1990. Cytokine-stimulated human immunodeficiency virus replication is inhibited by *N*-acetyl-L-cysteine. Proc. Natl. Acad. Sci. USA **87:**4884–4888.
47. **Saenz, D. T., W. Teo, J. C. Olsen, and E. M. Poeschla.** 2005. Restriction of feline immunodeficiency virus by Ref1, Lv1, and primate TRIM5α proteins. J. Virol. **79:**15175–15188.
48. **Sakurai, T., T. Kaise, and C. Matsubara.** 1998. Inorganic and methylated arsenic compounds induce cell death in murine macrophages via different mechanisms. Chem. Res. Toxicol. **11:**273–283.
49. **Sarcar, B., A. K. Ghosh, R. Steele, R. Ray, and R. B. Ray.** 2004. Hepatitis C virus NS5A mediated STAT3 activation requires co-operation of Jak1 kinase. Virology **322:**51–60.
50. **Sayah, D. M., and J. Luban.** 2004. Selection for loss of Ref1 activity in human cells releases human immunodeficiency virus type 1 from cyclophilin A dependence during infection. J. Virol. **78:**12066–12070.
51. **Shen, Z. X., G. Q. Chen, J. H. Ni, X. S. Li, S. M. Xiong, Q. Y. Qiu, J. Zhu, W. Tang, G. L. Sun, K. Q. Yang, Y. Chen, L. Zhou, Z. W. Fang, Y. T. Wang, J. Ma, P. Zhang, T. D. Zhang, S. J. Chen, Z. Chen, and Z. Y. Wang.** 1997. Use of arsenic trioxide (As_2O_3) in the treatment of acute promyelocytic leukemia (APL). II. Clinical efficacy and pharmacokinetics in relapsed patients. Blood **89:**3354–3360.
52. **Soignet, S. L., P. Maslak, Z. G. Wang, S. Jhanwar, E. Calleja, L. J. Dardashti, D. Corso, A. DeBlasio, J. Gabrilove, D. A. Scheinberg, P. P. Pandolfi, and R. P. Warrell, Jr.** 1998. Complete remission after treatment of acute promyelocytic leukemia with arsenic trioxide. N. Engl. J. Med. **339:**1341–1348.
53. **Staal, F. J. T., M. Roederer, L. A. Herzenberg, and L. A. Herzenberg.** 1990. Intracellular thiols regulate activation of nuclear factor κB and transcription of human immunodeficiency virus. Proc. Natl. Acad. Sci. USA **87:**9943–9947.
54. **Staal, F. J. T., S. W. Ela, M. Roederer, M. T. Anderson, L. A. Herzenberg, and L. A. Herzenberg.** 1992. Glutathione deficiency and human immunodeficiency virus infection. Lancet **339:**909–912.
55. **Tardif, K. D., K. Mori, and A. Siddiqui.** 2002. Hepatitis C virus subgenomic replicons induce endoplasmic reticulum stress activating an interacellular signaling pathway. J. Virol. **76:**7453–7459.
56. **Tavalai, N., P. Papior, S. Rechter, M. Leis, and T. Stamminger.** 2006. Evidence for a role of the cellular ND10 protein PML in mediating intrinsic immunity against human cytomegalovirus infections. J. Virol. **80:**8006–8018.
57. **Turelli, P., V. Doucas, E. Craig, B. Mangeat, N. Klages, R. Evans, G. Kalpana, and D. Trono.** 2001. Cytoplasmic recruitment of INI1 and PML on incoming HIV preintegration complexes: interference with early steps of viral replication. Mol. Cell **7:**1245–1254.
58. **Wakita, T., T. Pietschmann, T. Kato, T. Date, M. Miyamoto, Z. Zhao, K. Murthy, A. Habermann, H. G. Kräusslich, M. Mizokami, R. Bartenschlager, and T. J. Liang.** 2005. Production of infectious hepatitis C virus in tissue culture from a cloned viral genome. Nat. Med. **11:**791–796.
59. **Waris, G., J. Turson, T. Hassanein, and A. Siddiqui.** 2005. Hepatitis C virus (HCV) constitutively activates STAT-3 via oxidative stress: role of STAT3 in HCV replication. J. Virol. **79:**1569–1580.
60. **Waris, G., A. Livolsi, V. Imbert, J. F. Peyron, and A. Siddiqui.** 2003. Hepatitis C virus NS5A and subgenomic replicon activate NF-κB via tyrosine phosphorylation of IkBa and its degradation by calpain protease. J. Biol. Chem. **278:**40778–40787.
61. **Wen, F., M. Y. Abdalla, C. Aloman, J. Xiang, I. M. Ahmad, J. Walewski, M. L. McCormick, K. E. Brown, A. D. Branch, D. R. Spitz, B. E. Britigan, and W. N. Schmidt.** 2004. Increased prooxidant production and enhanced susceptibility to glutathione depletion in HepG2 cells co-expressing HCV core protein and CYP2E1. J. Med. Virol. **72:**230–240.
62. **Wetzler, M., M. T. Brady, E. Tracy, Z. R. Li, K. A. Donohue, K. L. O'Loughlin, Y. Cheng, A. Mortazavi, A. A. McDonald, P. Kunapuli, P. K. Wallace, M. R. Baer, J. K. Cowell, and H. Baumann.** 2006. Arsenic trioxide affects signal transducer and activator of transcription proteins through alteration of protein tyrosine kinase phosphorylation. Clin. Cancer Res. **12:** 6817–6825.

63. **Yang, S., C. Kuo, J. E. Bisi, and M. K. Kim.** 2002. PML-dependent apoptosis after DNA damage is regulated by the checkpoint kinase hCds1/Chk2. Nat. Cell Biol. **4**:865–870.
64. **Yang, S., J. H. Jeong, A. L. Brown, C. H. Lee, P. P. Pandolfi, J. H. Chung, and M. K. Kim.** 2006. Promyelocytic leukemia activates Chk2 by mediating Chk2 autophosphorylation. J. Biol. Chem. **281**:26645–26654.
65. **Yano, M., M. Ikeda, K. Abe, H. Dansako, S. Ohkoshi, Y. Aoyagi, and N. Kato.** 2007. Comprehensive analysis of the effects of ordinary nutrients on hepatitis C virus RNA replication in cell culture. Antimicrob. Agents Chemother. **51**:2016–2027.
66. **Yoda, A., K. Toyoshima, Y. Watanabe, N. Onishi, Y. Hazaka, Y. Tsukuda, J. Tsukada, T. Kondo, Y. Tanaka, and Y. Minami.** 2008. Arsenic trioxide augments Chk2/p53-mediated apoptosis by inhibiting oncogenic Wip1 phosphatase. J. Biol. Chem. **283**:18969–18979.
67. **Yoshida, T., T. Hanada, T. Tokuhisa, K. Kosai, M. Sata, M. Kohara, and A. Yoshimura.** 2002. Activation of STAT3 by the hepatitis C virus core protein leads to cellular transformation. J. Exp. Med. **196**:641–653.
68. **Zhang, P., S. Y. Wang, and X. H. Hu.** 1996. Arsenic trioxide treated 72 cases of acute promyelocytic leukemia. Chin. J. Hematol. **17**:58–62.
69. **Zhu, H., X. Shang, N. Terada, and C. Liu.** 2004. STAT3 induces anti-hepatitis C viral activity in liver cells. Biochem. Biophys. Res. Commun. **324**:518–528.
70. **Zhu, J., M. H. M. Koken, F. Quignon, M. K. Chelbi-Alix, L. Degos, Z. Y. Wang, Z. Chen, and H. de Thé.** 1997. Arsenic-induced PML targeting onto nuclear bodies: implications for the treatment of acute promyelocytic leukemia. Proc. Natl. Acad. Sci. USA **94**:3978–3983.
71. **Zufferey, R., D. Nagy, R. J. Mandel, L. Naldini, and D. Trono.** 1997. Multiply attenuated lentiviral vector achieves efficient gene delivery in vivo. Nat. Biotechnol. **15**:871–875.

JOURNAL OF VIROLOGY, Mar. 2009, p. 2389–2392 Vol. 83, No. 5
0022-538X/09/$08.00+0 doi:10.1128/JVI.01690-08

Proteasomal Turnover of Hepatitis C Virus Core Protein Is Regulated by Two Distinct Mechanisms: a Ubiquitin-Dependent Mechanism and a Ubiquitin-Independent but PA28γ-Dependent Mechanism▽

Ryosuke Suzuki,[1] Kohji Moriishi,[2] Kouichirou Fukuda,[1] Masayuki Shirakura,[1] Koji Ishii,[1] Ikuo Shoji,[3] Takaji Wakita,[1] Tatsuo Miyamura,[1] Yoshiharu Matsuura,[2] and Tetsuro Suzuki[1]*

Department of Virology II, National Institute of Infectious Diseases, Tokyo 162-8640,[1] Department of Molecular Virology, Research Institute for Microbial Diseases, Osaka University, Osaka 565-0871,[2] and Division of Microbiology, Kobe University Graduate School of Medicine, Hyogo 650-0017,[3] Japan

Received 8 August 2008/Accepted 5 December 2008

We have previously reported on the ubiquitylation and degradation of hepatitis C virus core protein. Here we demonstrate that proteasomal degradation of the core protein is mediated by two distinct mechanisms. One leads to polyubiquitylation, in which lysine residues in the N-terminal region are preferential ubiquitylation sites. The other is independent of the presence of ubiquitin. Gain- and loss-of-function analyses using lysineless mutants substantiate the hypothesis that the proteasome activator PA28γ, a binding partner of the core, is involved in the ubiquitin-independent degradation of the core protein. Our results suggest that turnover of this multifunctional viral protein can be tightly controlled via dual ubiquitin-dependent and -independent proteasomal pathways.

Hepatitis C virus (HCV) core protein, whose amino acid sequence is highly conserved among different HCV strains, not only is involved in the formation of the HCV virion but also has a number of regulatory functions, including modulation of signaling pathways, cellular and viral gene expression, cell transformation, apoptosis, and lipid metabolism (reviewed in references 9 and 15). We have previously reported that the E6AP E3 ubiquitin (Ub) ligase binds to the core protein and plays an important role in polyubiquitylation and proteasomal degradation of the core protein (22). Another study from our group identified the proteasome activator PA28γ/REG-γ as an HCV core-binding partner, demonstrating degradation of the core protein via a PA28γ-dependent pathway (16, 17). In this work, we further investigated the molecular mechanisms underlying proteasomal degradation of the core protein and found that in addition to regulation by the Ub-mediated pathway, the turnover of the core protein is also regulated by PA28γ in a Ub-independent manner.

Although ubiquitylation of substrates generally requires at least one Lys residue to serve as a Ub acceptor site (5), there is no consensus as to the specificity of the Lys targeted by Ub (4, 8). To determine the sites of Ub conjugation in the core protein, we used site-directed mutagenesis to replace individual Lys residues or clusters of Lys residues with Arg residues in the N-terminal 152 amino acids (aa) of the core (C152), within which is contained all seven Lys residues (Fig. 1A). Plasmids expressing a variety of mutated core proteins were generated by PCR and inserted into the pCAGGS (18). Each core-expressing construct was transfected into human embryonic kidney 293T cells along with the pMT107 (25) encoding a Ub moiety tagged with six His residues (His_6). Transfected cells were treated with the proteasome inhibitor MG132 for 14 h to maximize the level of Ub-conjugated core intermediates by blocking the proteasome pathway and were harvested 48 h posttransfection. His_6-tagged proteins were purified from the extracts by Ni^{2+}-chelation chromatography. Eluted protein and whole lysates of transfected cells before purification were analyzed by Western blotting using anticore antibodies (Fig. 1B). Mutations replacing one or two Lys residues with Arg in the core protein did not affect the efficiency of ubiquitylation: detection of multiple Ub-conjugated core intermediates was observed in the mutant core proteins comparable to the results seen with the wild-type core protein as previously reported (23). In contrast, a substitution of four N-terminal Lys residues (C152K6-23R) caused a significant reduction in ubiquitylation (Fig. 1B, lane 9). Multiple Ub-conjugated core intermediates were not detected in the Lys-less mutant (C152KR), in which all seven Lys residues were replaced with Arg (Fig. 1B, lane 11). These results suggest that there is not a particular Lys residue in the core protein to act as the Ub acceptor but that more than one Lys located in its N-terminal region can serve as the preferential ubiquitylation site. In rare cases, Ub is known to be conjugated to the N terminus of proteins; however, these results indicate that this does not occur within the core protein.

To investigate how polyubiquitylation correlates with proteasome degradation of the core protein, we performed kinetic analysis of the wild-type and mutated core proteins by use of the Ub protein reference (UPR) technique, which can compensate for data scatter of sample-to-sample variations such as levels of expression (10, 24). Fusion proteins expressed from UPR-based constructs (Fig. 2A) were cotranslationally cleaved by deubiquitylating enzymes, thereby generating equimolar quantities of the core proteins and the reference protein, dihydrofolate reductase-hemagglutinin (DHFR-HA) tag-modified Ub, in which the Lys at aa 48 was replaced by Arg to prevent its polyubiquitylation (Ub^{R48}). After 24 h of transfec-

* Corresponding author. Mailing address: Department of Virology II, National Institute of Infectious Diseases, 1-23-1 Toyama, Shinjuku-ku, Tokyo 162-8640, Japan. Phone: 81-3-5285-1111. Fax: 81-3-5285-1161. E-mail: tesuzuki@nih.go.jp.

▽ Published ahead of print on 17 December 2008.

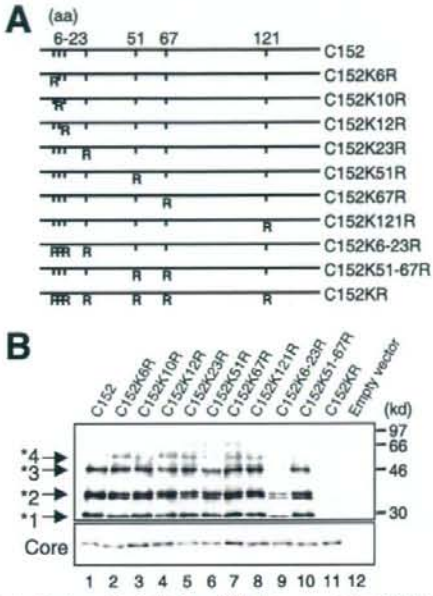

FIG. 1. In vivo ubiquitylation of HCV core protein. (A) The HCV core protein (N-terminal 152 aa) is represented on the top. The positions of the amino acid residues of the core protein are indicated above the bold lines. The positions of the seven Lys residues in the core are marked by vertical ticks. Substitution of Lys with Arg (R) is schematically depicted. (B) Detection of ubiquitylated forms of the core proteins. The transfected cells with core expression plasmids and pMT107 were treated with the proteasome inhibitor MG132 and harvested 48 h after transfection. His_6-tagged proteins were purified and subsequently analyzed by Western blot analysis using anticore antibody (upper panel). Core proteins conjugated to a number of His_6-Ub are denoted with asterisks. Whole lysates of transfected cells before purification were also analyzed (lower panel). Lanes 1 to 11, C152 to C152KR, as indicated for panel A. Lane 12; empty vector.

tion with UPR constructs, cells were treated with cycloheximide and the amounts of core proteins and DHFR-HA-Ub^{R48} at the indicated time points were determined by Western blot analysis using anticore and anti-HA antibodies. The mature form of the core protein, aa 1 to 173 (C173) (13, 20), and C152 were degraded with first-order kinetics (Fig. 2B and D). MG132 completely blocked the degradation of C173 and C152 (Fig. 2B), and C152K6-23R and C152KR were markedly stabilized (Fig. 2C). The half-lives of C173 and C152 were calculated to be 5 to 6 h, whereas those of C152K6-23R and C152KR were calculated to be 22 to 24 h (Fig. 2D), confirming that the Ub plays an important role in regulating degradation of the core protein. Nevertheless, these results also suggest possible involvement of the Ub-independent pathway in the turnover of the core protein, as C152KR is more destabilized than the reference protein (Fig. 2C and 2D).

We have shown that PA28γ specifically binds to the core protein and is involved in its degradation (16, 17). Recent studies demonstrated that PA28-γ is responsible for Ub-independent degradation of the steroid receptor coactivator SRC-3 and cell cycle inhibitors such as p21 (3, 11, 12). Thus, we next investigated the possibility of PA28γ involvement in the deg-

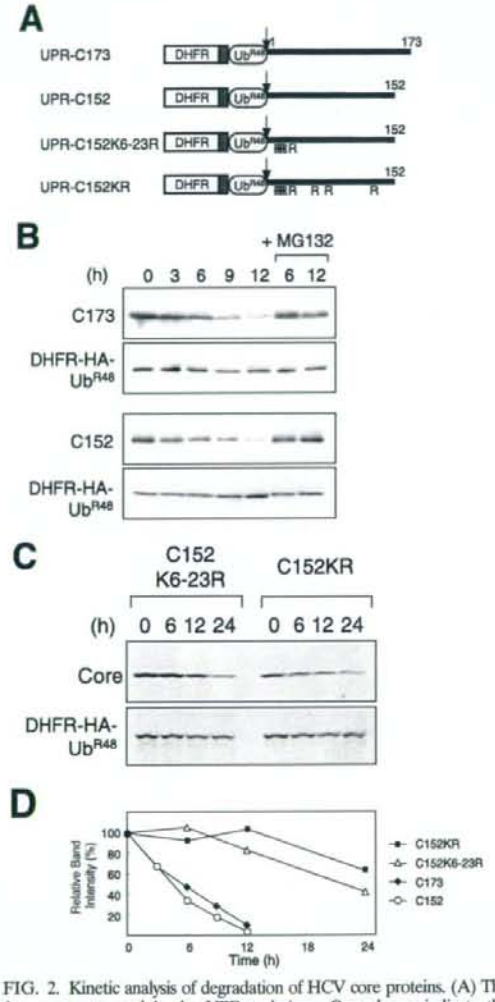

FIG. 2. Kinetic analysis of degradation of HCV core proteins. (A) The fusion constructs used in the UPR technique. Open boxes indicate the DHFR sequence, which is extended at the C terminus by a sequence containing the HA epitope (hatched boxes). Ub^{R48} moieties bearing the Lys-Arg substitution at aa 48 are represented by open ellipses. Bold lines indicate the regions of the core protein. The amino acid positions of the core protein are indicated above the bold lines. The arrows indicate the sites of in vivo cleavage by deubiquitylating enzymes. (B and C) Turnover of the core proteins. After a 24-h transfection with each UPR construct, cells were treated with 50 μg of cycloheximide/ml in the presence or absence of 10 μM MG132 for the different time periods indicated. Cells were lysed at the different time points indicated, followed by evaluation via sodium dodecyl sulfate-polyacrylamide gel electrophoresis and Western blot analysis using antibodies against the core protein and HA. (D) Quantitation of the data shown in panels B and C. At each time point, the ratio of band intensity of the core protein relative to the reference DHFR-HA-Ub^{R48} was determined by densitometry and is plotted as a percentage of the ratio at time zero.

radation of either C152KR or C152. Since C152KR carries two amino acid substitutions in the PA28γ-binding region (aa 44 to 71) (17), we tested the influence of the mutations of C152KR on the interaction with PA28γ by use of a coimmunoprecipi-

tation assay. When Flag-tagged PA28γ (F-PA28γ) was expressed in cells along with C152 or C152KR, F-PA28γ precipitated along with both C152 and C152KR, indicating that PA28γ interacts with both core proteins (Fig. 3A). Figure 3B reveals the effect of exogenous expression of F-PA28γ on the steady-state levels of C152 and C152KR. Consistent with previous data (17), the expression level of C152 was decreased to a nearly undetectable level in the presence of PA28γ (Fig. 3B, lanes 1 and 3). Interestingly, exogenous expression of PA28γ led to a marked reduction in the amount of C152KR expressed (Fig. 3B, lanes 5 and 7). Treatment with MG132 increased the steady-state level of the C152KR in the presence of F-PA28γ as well as the level of C152 (Fig. 3B, lanes 4 and 8).

We further investigated whether PA28γ affects the turnover of Lys-less core protein through time course experiments. C152KR was rapidly destabilized and almost completely degraded in a 3-h chase experiment using cells overexpressing F-PA28γ (Fig. 3C, left panels). A similar result was obtained using an analogous Lys-less mutant of the full-length core protein C191KR (Fig. 3C, right panels), thus demonstrating that the Lys-less core protein undergoes proteasomal degradation in a PA28γ-dependent manner. These results suggest that PA28γ may play a role in accelerating the turnover of the HCV core protein that is independent of ubiquitylation.

Finally, we examined gain- and loss-of-function of PA28γ with respect to degradation of full-length wild-type (C191) and mutated (C191KR) core proteins in human hepatoma Huh-7 cells. As expected, exogenous expression of PA28γ or E6AP caused a decrease in the C191 steady-state levels (Fig. 4A). In contrast, the C191KR level was decreased with expression of PA28γ but not of E6AP. We further used RNA interference to inhibit expression of PA28γ or E6AP. An increase in the abundance of C191KR was observed with PA28γ small interfering RNA (siRNA) but not with E6AP siRNA (Fig. 4B). An increase in the C191 level caused by the activity of siRNA against PA28γ or E6AP was confirmed as well.

Taking these results together, we conclude that turnover of the core protein is regulated by both Ub-dependent and Ub-independent pathways and that PA28γ is possibly involved in Ub-independent proteasomal degradation of the core protein. PA28 is known to specifically bind and activate the 20S proteasome (19). Thus, PA28γ may function by facilitating the delivery of the core protein to the proteasome in a Ub-independent manner.

Accumulating evidence suggests the existence of proteasome-dependent but Ub-independent pathways for protein degradation, and several important molecules, such as p53, p73, Rb, SRC-3, and the hepatitis B virus X protein, have two distinct degradation pathways that function in a Ub-dependent and Ub-independent manner (1, 2, 6, 7, 14, 21, 27). Recently, critical roles for PA28γ in the Ub-independent pathway have been demonstrated; SRC-3 and p21 can be recognized by the 20S proteasome independently of ubiquitylation through their interaction with PA28γ (3, 11, 12). It has also been reported that phosphorylation-dependent ubiquitylation mediated by GSK3 and SCF is important for SRC-3 turnover (26). Nevertheless, the precise mechanisms underlying turnover of most of the proteasome substrates that are regulated in both Ub-dependent and Ub-independent manners are not well understood. To our knowledge, the HCV core protein is the first

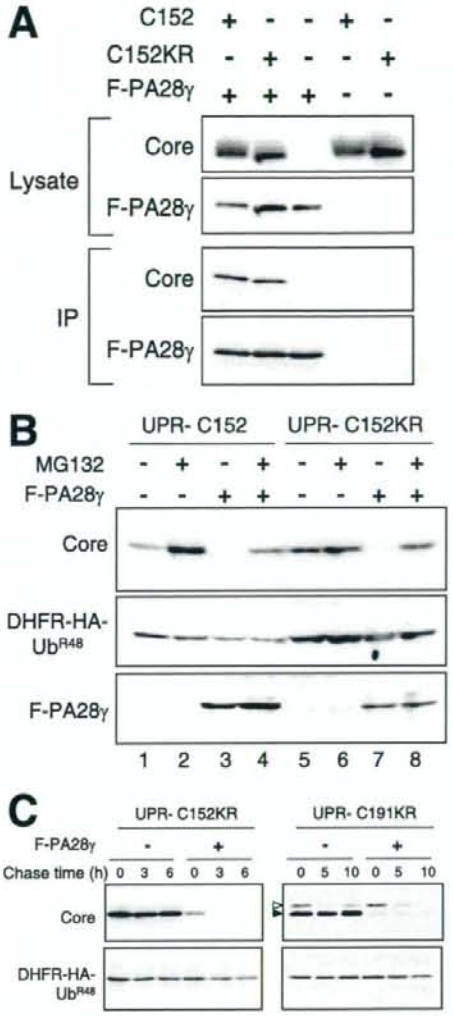

FIG. 3. PA28γ-dependent degradation of the core protein. (A) Interaction of the core protein with PA28γ. Cells were cotransfected with the wild-type (C152) or Lys-less (C152KR) core expression plasmid in the presence of a Flag-PA28γ (F-PA28γ) expression plasmid or an empty vector. The transfected cells were treated with MG132. After 48 h, the cell lysates were immunoprecipitated with anti-Flag antibody and visualized by Western blotting with anticore antibodies. Western blot analysis of whole cell lysates was also performed. (B) Degradation of the wild-type and Lys-less core proteins via the PA28γ-dependent pathway. Cells were transfected with the UPR construct with or without F-PA28γ. In some cases, cells were treated with 10 μM MG132 for 14 h before harvesting. Western blot analysis was performed using anticore, anti-HA, and anti-Flag antibodies. (C) After 24 h of transfection with UPR-C152KR and UPR-C191KR with or without F-PA28γ (an empty vector), cells were treated with 50 μg of cycloheximide/ml for different time periods as indicated (chase time). Western blot analysis was performed using anticore and anti-HA antibodies. The precursor core protein and the core that was processed, presumably by signal peptide peptidase, are denoted by open and closed triangles, respectively.

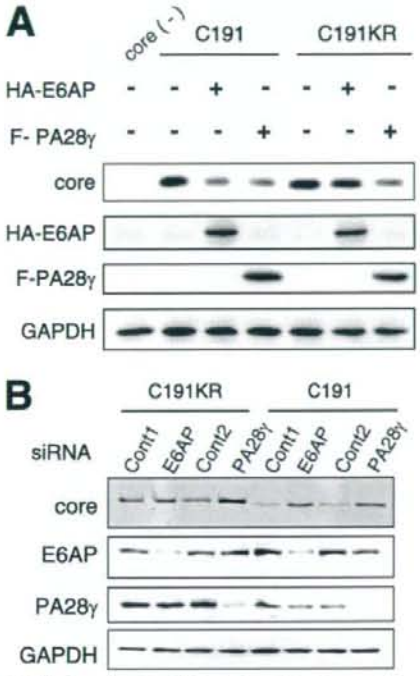

FIG. 4. Ub-dependent and Ub-independent degradation of the full-length core protein in hepatic cells. (A) Huh-7 cells were cotransfected with plasmids for the full-length core protein (C191) or its Lys-less mutant (C191KR) in the presence of F-PA28γ or HA-tagged-E6AP expression plasmid (HA-E6AP). After 48 h, cells were lysed and Western blot analysis was performed using anticore, anti-HA, anti-Flag, or anti-GAPDH. (B) Huh-7 cells were cotransfected with core expression plasmids along with siRNA against PA28γ or E6AP or with negative control siRNA. Cells were harvested 72 h after transfection and subjected to Western blot analysis.

viral protein studied that has led to identification of key cellular factors responsible for proteasomal degradation via dual distinct mechanisms. Although the question remains whether there is a physiological significance of the Ub-dependent and Ub-independent degradation of the core protein, it is reasonable to consider that tight control over cellular levels of the core protein, which is multifunctional and essential for viral replication, maturation, and pathogenesis, may play an important role in representing the potential for its functional activity.

This work was supported by a grant-in-aid for Scientific Research from the Japan Society for the Promotion of Science, from the Ministry of Health, Labor and Welfare of Japan, and from the Ministry of Education, Culture, Sports, Science and Technology, by Research on Health Sciences focusing on Drug Innovation from the Japan Health Sciences Foundation, Japan, and by the Program for Promotion of Fundamental Studies in Health Sciences of the National Institute of Biomedical Innovation of Japan.

REFERENCES

1. **Asher, G., J. Lotem, L. Sachs, C. Kahana, and Y. Shaul.** 2002. Mdm-2 and ubiquitin-independent p53 proteasomal degradation regulated by NQO1. Proc. Natl. Acad. Sci. USA **99:**13125–13130.
2. **Asher, G., P. Tsvetkov, C. Kahana, and Y. Shaul.** 2005. A mechanism of ubiquitin-independent proteasomal degradation of the tumor suppressors p53 and p73. Genes Dev. **19:**316–321.
3. **Chen, X., L. F. Barton, Y. Chi, B. E. Clurman, and J. M. Roberts.** 2007. Ubiquitin-independent degradation of cell-cycle inhibitors by the REGγ proteasome. Mol. Cell **26:**843–852.
4. **Ciechanover, A.** 1998. The ubiquitin-proteasome pathway: on protein death and cell life. EMBO J. **17:**7151–7160.
5. **Hershko, A., A. Ciechanover, and A. Varshavsky.** 2000. The ubiquitin system. Nat. Med. **6:**1073–1081.
6. **Jariel-Encontre, I., M. Pariat, F. Martin, S. Carillo, C. Salvat, and M. Piechaczyk.** 1995. Ubiquitinylation is not an absolute requirement for degradation of c-Jun protein by the 26 S proteasome. J. Biol. Chem. **270:**11623–11627.
7. **Jin, Y., H. Lee, S. X. Zeng, M. S. Dai, and H. Lu.** 2003. MDM2 promotes p21waf1/cip1 proteasomal turnover independently of ubiquitylation. EMBO J. **22:**6365–6377.
8. **Ju, D., and Y. Xie.** 2006. Identification of the preferential ubiquitination site and ubiquitin-dependent degradation signal of Rpn4. J. Biol. Chem. **281:**10657–10662.
9. **Lai, M. M. C., and C. F. Ware.** 1999. Hepatitis C virus core protein: possible roles in viral pathogenesis. Springer, Berlin, Germany.
10. **Lévy, F., N. Johnsson, T. Rumenapf, and A. Varshavsky.** 1996. Using ubiquitin to follow the metabolic fate of a protein. Proc. Natl. Acad. Sci. USA **93:**4907–4912.
11. **Li, X., L. Amazit, W. Long, D. M. Lonard, J. J. Monaco, and B. W. O'Malley.** 2007. Ubiquitin- and ATP-independent proteolytic turnover of p21 by the REGγ-proteasome pathway. Mol. Cell **26:**831–842.
12. **Li, X., D. M. Lonard, S. Y. Jung, A. Malovannaya, Q. Feng, J. Qin, S. Y. Tsai, M. J. Tsai, and B. W. O'Malley.** 2006. The SRC-3/AIB1 coactivator is degraded in a ubiquitin- and ATP-independent manner by the REGγ proteasome. Cell **124:**381–392.
13. **Liu, Q., C. Tackney, R. A. Bhat, A. M. Prince, and P. Zhang.** 1997. Regulated processing of hepatitis C virus core protein is linked to subcellular localization. J. Virol. **71:**657–662.
14. **Lonard, D. M., Z. Nawaz, C. L. Smith, and B. W. O'Malley.** 2000. The 26S proteasome is required for estrogen receptor-α and coactivator turnover and for efficient estrogen receptor-α transactivation. Mol. Cell **5:**939–948.
15. **Moradpour, D., F. Penin, and C. M. Rice.** 2007. Replication of hepatitis C virus. Nat. Rev. Microbiol. **5:**453–463.
16. **Moriishi, K., R. Mochizuki, K. Moriya, H. Miyamoto, Y. Mori, T. Abe, S. Murata, K. Tanaka, T. Miyamura, T. Suzuki, K. Koike, and Y. Matsuura.** 2007. Critical role of PA28γ in hepatitis C virus-associated steatogenesis and hepatocarcinogenesis. Proc. Natl. Acad. Sci. USA **104:**1661–1666.
17. **Moriishi, K., T. Okabayashi, K. Nakai, K. Moriya, K. Koike, S. Murata, T. Chiba, K. Tanaka, R. Suzuki, T. Suzuki, T. Miyamura, and Y. Matsuura.** 2003. Proteasome activator PA28γ-dependent nuclear retention and degradation of hepatitis C virus core protein. J. Virol. **77:**10237–10249.
18. **Niwa, H., K. Yamamura, and J. Miyazaki.** 1991. Efficient selection for high-expression transfectants with a novel eukaryotic vector. Gene **108:**193–199.
19. **Realini, C., C. C. Jensen, Z. Zhang, S. C. Johnston, J. R. Knowlton, C. P. Hill, and M. Rechsteiner.** 1997. Characterization of recombinant REGα, REGβ, and REGγ proteasome activators. J. Biol. Chem. **272:**25483–25492.
20. **Santolini, E., G. Migliaccio, and N. La Monica.** 1994. Biosynthesis and biochemical properties of the hepatitis C virus core protein. J. Virol. **68:**3631–3641.
21. **Sheaff, R. J., J. D. Singer, J. Swanger, M. Smitherman, J. M. Roberts, and B. E. Clurman.** 2000. Proteasomal turnover of p21Cip1 does not require p21Cip1 ubiquitination. Mol. Cell **5:**403–410.
22. **Shirakura, M., K. Murakami, T. Ichimura, R. Suzuki, T. Shimoji, K. Fukuda, K. Abe, S. Sato, M. Fukasawa, Y. Yamakawa, M. Nishijima, K. Moriishi, Y. Matsuura, T. Wakita, T. Suzuki, P. M. Howley, T. Miyamura, and I. Shoji.** 2007. E6AP ubiquitin ligase mediates ubiquitylation and degradation of hepatitis C virus core protein. J. Virol. **81:**1174–1185.
23. **Suzuki, R., K. Tamura, J. Li, K. Ishii, Y. Matsuura, T. Miyamura, and T. Suzuki.** 2001. Ubiquitin-mediated degradation of hepatitis C virus core protein is regulated by processing at its carboxyl terminus. Virology **280:**301–309.
24. **Suzuki, T., and A. Varshavsky.** 1999. Degradation signals in the lysine-asparagine sequence space. EMBO J. **18:**6017–6026.
25. **Treier, M., L. M. Staszewski, and D. Bohmann.** 1994. Ubiquitin-dependent c-Jun degradation in vivo is mediated by the δ domain. Cell **78:**787–798.
26. **Wu, R. C., Q. Feng, D. M. Lonard, and B. W. O'Malley.** 2007. SRC-3 coactivator functional lifetime is regulated by a phospho-dependent ubiquitin time clock. Cell **129:**1125–1140.
27. **Zhang, Z., and R. Zhang.** 2008. Proteasome activator PA28γ regulates p53 by enhancing its MDM2-mediated degradation. EMBO J. **27:**852–864.

Virology 383 (2009) 319–327

Contents lists available at ScienceDirect

Virology

journal homepage: www.elsevier.com/locate/yviro

Cellular vimentin content regulates the protein level of hepatitis C virus core protein and the hepatitis C virus production in cultured cells

Yuko Nitahara-Kasahara [a,1], Masayoshi Fukasawa [a,*], Fumiko Shinkai-Ouchi [a], Shigeko Sato [a], Tetsuro Suzuki [b], Kyoko Murakami [b], Takaji Wakita [b], Kentaro Hanada [a], Tatsuo Miyamura [c], Masahiro Nishijima [a,d]

[a] Department of Biochemistry and Cell Biology, National Institute of Infectious Diseases, 1-23-1, Toyama, Shinjuku-ku, Tokyo 162-8640, Japan
[b] Department of Virology II, National Institute of Infectious Diseases, Tokyo 162-8640, Japan
[c] National Institute of Infectious Diseases, Tokyo 162-8640, Japan
[d] National Institute of Health Sciences, Tokyo 158-8501, Japan

ARTICLE INFO

Article history:
Received 14 August 2008
Returned to author for revision
3 September 2008
Accepted 6 October 2008
Available online 14 November 2008

Keywords:
Hepatitis C virus
Core protein
Vimentin

ABSTRACT

Hepatitis C virus (HCV) core protein is essential for virus particle formation. Using HCV core-expressing and non-expressing Huh7 cell lines, Uc39-6 and Uc321, respectively, we performed comparative proteomic studies of proteins in the 0.5% Triton X-100-insoluble fractions of cells, and found that core-expressing Uc39-6 cells had much lower vimentin content than Uc321 cells. In experiments using vimentin-overexpressing and vimentin-knocked-down cells, we demonstrated that core protein levels were affected by cellular vimentin content. When vimentin expression was knocked-down, there was no difference in mRNA level of core protein; but proteasome-dependent degradation of the core protein was strongly reduced. These findings suggest that the turnover rate of core protein is regulated by cellular vimentin content. HCV production was also affected by cellular vimentin content. Our findings together suggest that modulation of hepatic vimentin expression might enable the control of HCV production.

Introduction

Hepatitis C virus (HCV) is a major causative agent of chronic hepatitis (Choo et al., 1989; Kuo et al., 1989). Persistent HCV infection, which develops in at least 70% of infected patients, is strongly correlated with the development of severe liver diseases such as fibrosis, steatosis, cirrhosis, and hepatocellular carcinomas (HCC). Since more than 170 million people in the world are currently infected with HCV (Choo et al., 1989) and there is no treatment completely effective in curing HCV, HCV infection is one of the most important global public health issues. Understanding of the life cycle of HCV and the mechanism by which HCV induces serious liver diseases is crucial for the development of novel anti-HCV strategies.

HCV is an RNA virus of the *Flaviviridae* family and possesses a single-stranded, positive-sense RNA genome of ~9.6 kb (Bartenschlager and Lohmann, 2000). The HCV RNA genome encodes a polyprotein of ~3000 amino acids that is processed by host and viral proteases into 10 individual components including 4 structural and 6 nonstructural proteins (reviewed by Reed and Rice, 2000). HCV core protein is crucial for virus particle production as the structural component of the viral nucleocapsid and as a unit required for formation of the active HCV replication/assembly complex in host cells (Boulant et al., 2007; Miyanari et al., 2007). In addition, the core protein plays pivotal roles in the pathogenesis of HCV infection, as suggested by the finding that transgenic mice expressing core protein in the liver tend to develop liver steatosis with subsequent HCC (Moriya et al., 1998; Moriya et al., 1997). A large number of studies have revealed that a variety of host proteins interact with the core protein (Suzuki et al., 2007). Although these interactions can markedly affect various biological functions in host cells, it is not clearly known yet which interactions and molecules play roles in HCV production or its pathogenicity. Recent exhaustive gene-silencing analyses of host factors using RNAi demonstrated that RNA helicase DDX3, one of the proteins that interacts with the core, is required for HCV RNA replication as well as HCV production (Ariumi et al., 2007; Randall et al., 2007).

In host hepatic cells, HCV core protein is distributed preferentially in the detergent-resistant fractions (Matto et al., 2004), and HCV RNA replication also occurs on detergent-resistant membranes (Aizaki et al., 2004; Shi et al., 2003), suggesting that host factors in the detergent-resistant fractions play roles in core protein functions. In this study, we focused on HCV core protein and the detergent-insoluble proteins of host cells, and performed comparative targeted proteomic analysis of the detergent-insoluble proteins in HCV core-expressing and non-expressing hepatic cells. We identified vimentin as a protein the amount of which was reduced in core-expressing cell lines, and demonstrated that cellular vimentin content affects levels of HCV core protein through the proteasome-mediated protein

* Corresponding author. Fax: +81 3 5285 1157.
E-mail address: fuka@nih.go.jp (M. Fukasawa).
[1] Present address: National Institute of Neuroscience, National Center of Neurology and Psychiatry, Tokyo 187-8502, Japan.

0042-6822/$ – see front matter © 2008 Published by Elsevier Inc.
doi:10.1016/j.virol.2008.10.009

degradation system. Since cellular vimentin levels ultimately affected HCV production, vimentin may be a novel target for strategies of anti-HCV treatment.

Results

Proteomic analysis of detergent-insoluble fractions (DISFs) by second-dimensional polyacrylamide gel electrophoresis (2D-PAGE)/MALDI-QIT-TOF MS

DISFs and detergent-soluble fractions (DSFs) were prepared from HCV core-expressing Uc39-6 and non-expressing Uc321 cells by a sucrose density gradient ultracentrifugation method as described in Materials and methods. Proteins in the DISFs and DSFs were analyzed by immunoblotting with antibodies to HCV core protein and various organelle markers (Fig. 1A). A significant amount of HCV core protein (~70%) was distributed in the DISF of Uc39-6 cells. Nuclear proteins such as laminA/C and laminB were concentrated only in the DISFs of both types of cells, whereas other organelle proteins such as annexin II (plasma membrane), fatty acid synthase (cytosol), prohibitin (mitochondria), and calnexin (endoplasmic reticulum) were detected in the DSFs but not DISFs (Fig. 1A), suggesting that the DISFs in both types of cells contain minor (~15%) discrete populations of cellular proteins. Next, we performed 2D-PAGE analysis of the DISFs in Uc321 and Uc39-6 cells. Proteins in the DISFs were separated by isoelectric focusing (IEF) (pH 4–7) and 12% sodium dodecyl sulfate (SDS)-PAGE, and visualized by SYPRO-Ruby staining (Fig. 1B). Intensity of each spot in 2-D images was compared between Uc321 and Uc39-6 cells. The most difference in DISF proteins between Uc321 and Uc39-6 cells (the Uc39-6/Uc321 ratios of intensity normalized with actin: 10.8–28.0) was detected in the spots numbered as 1 in Fig. 1B (MW~57 kDa, pI~4.7), in which vimentin alone was identified by mass spectrometric analysis. We therefore focused on the relationship between cellular vimentin and core protein in further investigations.

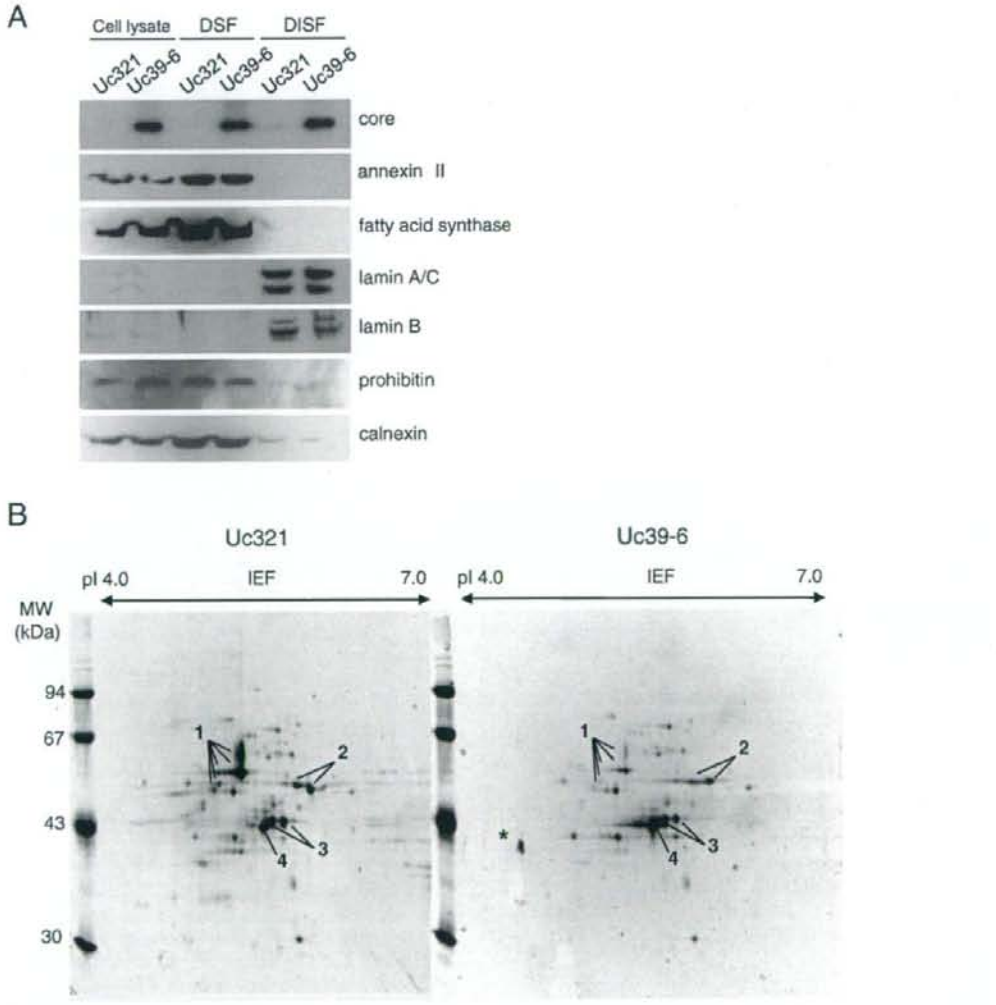

Fig. 1. Immunoblot and 2D-PAGE analysis of DISFs. (A) Total cell lysate fractions (5 μg of protein), DSFs (50 μg of protein), and DISFs (5 μg of protein) from core-expressing Uc39-6 and non-expressing Uc321 cells were analyzed by immunoblotting with antibodies to HCV core protein and various organelle markers as indicated. (B) 2D-PAGE analysis of proteins in DISFs of Uc321 and Uc39-6 cells. Proteins (150 μg) were separated by IEF (pH 4–7), followed by SDS-PAGE on a 12% gel. The gels were stained with SYPRO-Ruby. Major spots, identified as cytoskeletal proteins, are marked: 1, vimentin; 2, cytokeratin 8; 3, cytokeratin 18; 4, actin. *: a non-specific spot.

HCV core-expressing cell lines exhibited reduced vimentin content

To confirm the reduction of vimentin levels in DISFs of HCV core-expressing Uc39-6 cells, immunoblot analysis was performed using anti-vimentin antibody. Uc39-6 cells exhibited lower vimentin contents not only in DISF but also the total cell lysate fraction compared with control Uc321 cells (Fig. 2A). Similar results were obtained in the cell lysate fraction of another independent clone of an HCV core-expressing Huh7 cell line, Uc39-2 (Fig. 2B). Furthermore, a core-expressing hepatic HepG2 cell line, Hep39, also had lower vimentin content than a control cell line, Hepswx (Fig. 2C). These findings exclude the possibility that the reduction of vimentin levels in core-expressing cell lines is a clone- or cell-specific event. Consistent with these findings, levels of vimentin mRNA in Uc39-2 and Uc39-6 cells were also lower than that in Uc321 cells (data not shown). Taken together, these findings demonstrate marked reduction of vimentin expression in HCV core-expressing cell lines.

Cellular vimentin content affects the protein level of HCV core protein

To investigate the relationship between HCV core protein and vimentin, we examined the effect of cellular vimentin content on level of HCV core protein. When the expression of vimentin or control hypoxanthine guanine phosphoribosyltransferase 1 (HPRT) was knocked down in Uc39-6 cells by siRNA treatment, the protein level of HCV core protein in vimentin-knocked-down cells was significantly higher than those in siRNA-untreated and HPRT-knocked-down cells (Fig. 3A). On the other hand, cellular mRNA levels of HCV core protein, corrected for β-actin mRNA content, did not differ substantially among these types of cells (Table 1). These findings revealed that post-translational steps were involved in the increase of HCV core protein level in vimentin-knocked-down cells. Next, we established a vimentin-overexpressing Huh7 cell line, Huh7/vimentin, and compared the level of the core protein in Huh7/vimentin cells with that in control Huh7/hygro cells after transient expression of the core protein with pcEF39neo vector. After 9-day culture with G418 selection, the viabilities of the two types of cells were similar, though the level of expression of the core protein in Huh7/vimentin was significantly lower than that in Huh7/hygro cells (Fig. 3B). These findings demonstrated that level of HCV core protein was inversely correlated with cellular vimentin content, and thus strongly suggested that it was affected by cellular vimentin content.

We further attempted to verify these effects of vimentin using the vimentin-null cell line 1HF5 and the vimentin-expressing control cell line 2CB5, derived from human adrenal carcinoma SW13 cells (Sarria et al., 1990). When 1HF5 and 2CB5 cells were transfected with the core expression vector pcEF39neo and cultured with G418 selection, the viabilities of the two types of cells were similar, though the level of expression of the core protein in 1HF5 cells was much higher than that in 2CB5 cells (Fig. 3C), consistent with the results in Figs. 3A, B. An exogenously vimentin-expressing 1HF5 cell line carrying pcDNA3.1/Hygro/vimentin, 1HF5/vimentin, and a control vimentin-null cell line carrying pcDNA3.1/Hygro, 1HF5/hygro, were then established, and transfected with the green fluorescent protein (GFP)-expressing pcDNA3.1/EGFP vector, the core-coding pcEF39neo vector, or the control pcFE321swxneo vector. After selection under G418 for 9 days, the viabilities of these transfected cells were nearly the same. The levels of expression of GFP were similar in 1HF5/hygro and 1HF5/vimentin cells, while the core protein level in 1HF5/vimentin cells was significantly lower than that in 1HF5/hygro cells (Fig. 3D), consistent with the results in Fig. 3B.

These findings together indicate that cellular vimentin content regulates the level of HCV core protein in post-translational fashion.

Vimentin is involved in proteasomal degradation of core proteins in cells

HCV core proteins are known to be preferentially degraded by the proteasome-dependent pathway (Suzuki et al., 2001). To determine whether cellular vimentin content affects proteasome-dependent degradation of the core protein, we examined the effects of the proteasome inhibitor MG132 on core protein levels in vimentin-knocked-down cells. After Huh7 cells transfected with pCAG/Flag-core (Huh7/Flag-core cells) had been treated with MG132 for 16 h, cellular accumulation of core protein was analyzed by immunoblot (Fig. 4; lanes 3 vs 4), which indicated substantial proteasomal degradation of the core proteins in cultured cells, as described previously (Hope and McLauchlan, 2000; McLauchlan et al., 2002; Suzuki et al., 2001). Huh7/Flag-core cells transfected with control and HPRT siRNA duplexes exhibited similar increases in core protein levels by treatment with MG132 (Fig. 4; lanes 5 vs 6, and 9 vs 10). On the other hand, vimentin-knocked-down Huh7/Flag-core cells that were transfected with vimentin siRNA duplexes exhibited higher content of core protein (lane 7) than the other siRNA-treated cells (lanes 5 and 9), and MG132 treatment resulted in no significant difference in core protein levels in vimentin-knocked-down cells (lanes 7 and 8), indicating that proteasomal degradation of core proteins was markedly inhibited in the vimentin-knocked-down cells. These observations strongly suggested that vimentin plays an important role in the proteasome-mediated proteolytic pathway of the HCV core protein.

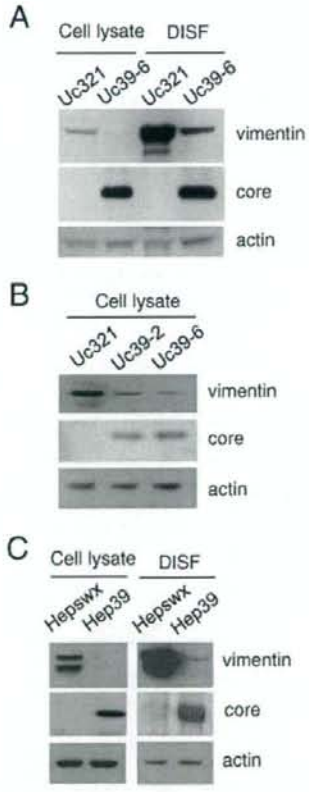

Fig. 2. Immunoblot analysis of vimentin in HCV core-expressing cell lines. Cell lysate fractions and DISFs from various cell lines were analyzed by immunoblotting with antibodies to vimentin, HCV core protein, and β-actin as indicated: cell lysate fractions and DISFs from Uc321 and Uc39-6 cells in (A), cell lysate fractions from Uc321, Uc39-2, and Uc39-6 cells in (B), and cell lysate fractions and DISFs from Hepswx and Hep39 cells in (C). Amounts of protein loaded were 18 μg in (A) and (B), and 5 μg in (C).

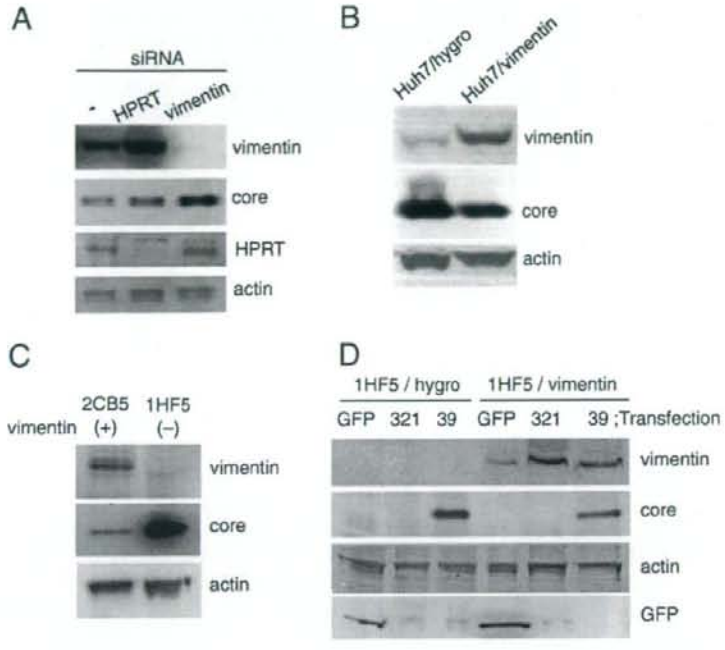

Fig. 3. Effects of cellular vimentin content on the level of expression of HCV core protein. Cellular level of expression of vimentin, HCV core protein, HPRT, β-actin, and GFP were analyzed by immunoblotting of total cell lysates (40 μg of protein) from various cells using specific antibodies. (A) Uc39-6 cells were transfected twice with a 2-day interval without (–) or with vimentin or control HPRT siRNA duplexes. Four days after the first transfection, cell lysates were collected and analyzed. (B) Huh7/hygro and Huh7/vimentin cells were transfected with the core protein-expression vector pcEF39neo, and selected under 1 mg/ml of G418 for 9 days. (C) The 2CB5 (vimentin+) and 1HF5 (vimentin−) lines of SW13 cells were transfected with pcEF39neo, and selected under 1 mg/ml of G418 for a week, followed by additional 2-week culture in normal culture medium. (D) 1HF5/hygro and 1HF5/vimentin cells were transfected with pcDNA3.1/EGFP (GFP), pcFE321swxneo (321), or pcEF39neo (39), and selected under 1 mg/ml of G418 for 9 days.

Under the various siRNA-treated conditions in Fig. 4, we also examined the protein levels of p53, one of the endogeneous host proteins the degradation of which is mainly regulated by proteasomal system (Morimoto et al., 2008). The pattern of p53 protein levels was very similar to that of core protein levels (Fig. 4), suggesting that the vimentin-dependent proteasomal degradation is not specific for the viral core protein. Vimentin-dependent proteasomal degradation system might be generally important for the turnover of endogeneous cellular proteins as well as the viral core protein.

Cellular vimentin contents affect HCV production

Since the level of expression of HCV core protein was affected by cellular vimentin content, we examined whether HCV production was also affected by cellular vimentin content. Infectious HCV (JFH1 strain) particles were used for the following infection assays. HCV production activity was determined by quantification of HCV core protein levels in the infected cells and culture supernatants. We first tested the effect of vimentin knockdown on HCV production. Examination of HCV-infected Huh7 cells treated with vimentin siRNA revealed higher amounts of HCV core protein in both cells and culture medium than examination of non-treated and control HPRT siRNA-treated cells (Fig. 5A). To examine whether the core protein levels in the cell-cultured media reflect the content of infectious HCV particles in them, Huh7 cells were treated with cell-cultured medium containing equal amounts (1.4 fmol) of the core protein collected from each type of cell described in Fig. 5A, and cellular levels of production of the core protein were determined by immunoblot analysis. They were nearly the same among the cells treated with each culture medium (Fig. 5B). These findings indicated that reduction of vimentin expression in Huh7 cells leads to more active HCV production and enhanced release to the supernatant.

We next examined the effects of vimentin overexpression on HCV production. When vimentin-overexpressing Huh7/vimentin and control Huh7/hygro cells were infected with HCV particles, Huh7/vimentin cells exhibited lower amounts of intracellular and extracellular HCV core protein than Huh7/hygro cells (Fig. 5C). Consistent with the results in Fig. 5A, these findings suggested that higher expression of vimentin in host cells resulted in lower HCV production.

We also examined the effect of vimentin knockdown on HCV RNA replication using a JFH1-subgenomic replicon (Fig. 5D). There were no significant differences in replication activities between vimentin-knocked-down cells and the other control cells. These findings indicated that cellular level of vimentin has no effects on HCV non-structural proteins which serve as a unit of RNA replication machinery of HCV. Collectively, these results demonstrated that HCV production activity but not HCV-RNA replication was inversely correlated with cellular vimentin content.

Table 1
mRNA levels of HCV core protein and β-actin in vimentin-knocked-down Uc39-6 cells

	siRNA		
	–	HPRT	vimentin
HCV core ($\times 10^4$ copies/μg total RNA)	2.9±0.3	1.7±0.1	3.0±0.2
β-actin ($\times 10^7$ copies/μg total RNA)	3.0±0.1	1.4±0.1	2.3±0.0
HCV core/β-actin[a]	1	1.3	1.3

Total RNA was isolated from Uc39-6 cells that had been treated twice with a 2-day interval with HPRT siRNA duplexes, with vimentin siRNA duplexes or without (–) either of them, and cultured for 4 days. mRNA levels of HCV core protein and β-actin (a control housekeeping gene) were determined by quantitative real-time PCR. Values are the mean±SD for three determinations.

[a] Numbers represent the relative amounts of HCV core protein mRNA normalized to β-actin level.

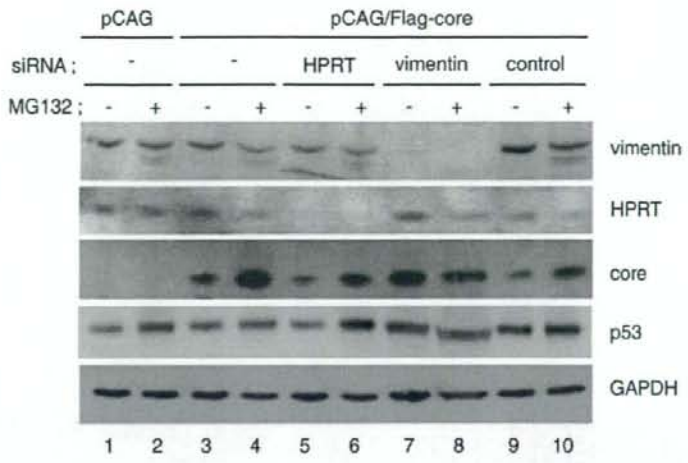

Fig. 4. Effects of the proteasome inhibitor MG132 on level of expression of HCV core protein in Huh7 cells. siRNA duplexes of control, HPRT, or vimentin, together with the core protein-expression vector pCAG/Flag-core, were transfected into Huh7 cells. After 2 days, transfection of these siRNAs was repeated. Cells were further cultured for 2 days and treated with (+) or without (−) MG132 (50 μM) for 16 h. Equivalent amounts of cell lysates were analyzed by immunoblotting with antibodies to vimentin, HPRT, core protein, p53, and GAPDH.

Furthermore, expression of vimentin and HCV core protein in Huh7 cells after HCV infection was observed by immunofluorescence microscopy (Fig. 5E), and the fluorescent intensity of vimentin in core-positive and core-negative Huh7 cells under HCV-infected conditions was determined (Fig. 5F). HCV-infected cells stained with the core-specific antibody always had lower vimentin content (Figs. 5E, F). Moreover, as shown in Fig. 5F, HCV core-negative cells exhibited more variable vimentin levels, whereas the core-positive cells had vimentin levels within a narrow range. These observations, which showed that a Huh7 cell population with lower vimentin content can preferentially produce HCV, were consistent with the results shown in Figs. 5A, C.

Finally, we examined the effects of MG132 on HCV core protein levels in HCV-infected cells in which vimentin was knocked-down or overexpressed. In the presence of MG132, non-treated and control HPRT siRNA-treated cells showed the significant increase of cellular HCV core protein levels, whereas vimentin-knocked-down cells did not (Fig. 5G). These results were consistent with those using HCV core-expressing cells (Fig. 4). HCV core content in vimentin-overexpressing Huh7/vimentin cells was lower than that in control Huh7/hygro cells, but after MG132 treatment Huh7/vimentin and Huh7/hygro cells showed the similar HCV core protein levels (Fig. 5H). Taken together, these results demonstrated the significant involvement of vimentin in proteasome-dependent degradation of HCV core protein in HCV-infected cells (Figs. 5G, H), as well as in HCV core-expressing cells (Fig. 4).

Discussion

By comparative proteomic analysis of the detergent-insoluble proteins in HCV core-expressing and non-expressing Huh7 cell lines, vimentin, an intermediate filament protein, was identified as the protein with the most dramatic reduction in level in the detergent-insoluble fraction of HCV core-expressing Uc39-6 cells (Figs. 1B and 2). On the other hand, there were no significant differences in the amounts of other major proteins including cytoskeletal components such as actin and cytokeratin 8/18 in the detergent-insoluble fractions between the core-expressing and non-expressing cells (Fig. 1B). These findings, together with similar results for other core-expressing cells (Fig. 2), suggested the existence of a specific relationship between the core protein and cellular vimentin. Consistent with these findings, immunofluorescence microscopic analysis of core-expressing cells (data not shown) and HCV-infected cells (Figs. 5E, F) showed that cells with intrinsic lower amount of vimentin are more permissive for higher HCV core protein content.

Knockdown of vimentin expression by siRNA treatment resulted in an increase in HCV core protein levels (Fig. 3A), while overexpression of vimentin reduced core protein contents (Fig. 3B). Similar results were obtained in the experiments using the vimentin-null cell line 1HF5 derived from SW13 cells (Figs. 3C and D). On the other hand, transient knockdown and overexpression of the core proteins in Uc39-6 and Huh7 cells, respectively, did not result in differences in cellular vimentin content (data not shown). These findings indicated that cellular vimentin level affects the level of expression of the core protein but not vice versa. Although transient expression of the core protein did not affect cellular vimentin content, why do various stable cell lines expressing the core protein have lower vimentin level? Since it was very hard to establish the cells stably expressing the core protein, we speculate that only the minor cell population innately having lower vimentin content was able to maintain the substantial core expression levels and was therefore selected.

We next demonstrated that vimentin affects core protein levels in post-translational fashion (Table 1) and is required for the proteasomal degradation of core protein in core-expressing cells (Fig. 4) and also in HCV-infected cells (Figs. 5G, H). Many studies with proteasome inhibitors have shown that a major pathway of degradation of core protein is mediated by the proteasomal system (Hope and McLauchlan, 2000; McLauchlan et al., 2002; Moriishi et al., 2003; Suzuki et al., 2001). PA28γ, a REG family proteasome activator also known as REGγ and Ki antigen, which is located in the nucleus, was shown to play an important role in the proteasomal degradation of the core protein (Moriishi et al., 2003). It was recently reported that the ubiquitin ligase E6AP, which is distributed in the perinuclear cytoplasm and colocalized with the core protein, is also involved in ubiquitylation and degradation of core protein (Shirakura et al., 2007). Vimentin filaments extend from the nuclear membrane toward the cell periphery. In addition, vimentin is known to colocalize with ubiquitinated protein aggregates and form aggresomes when the capacity of the proteasome is exceeded (Johnston et al., 1998). Pull-down assays against the core protein in core-expressing Huh7 cells indicated that a minor portion of cellular vimentin can interact with HCV core protein (data not shown), as